

UNCLASSIFIED

AD NUMBER
ADB244408
NEW LIMITATION CHANGE
TO Approved for public release, distribution unlimited
FROM Distribution: Further dissemination only as directed by Defense Nuclear Agency, 6801 Telegraph Rd., Alexandria, VA 22310-3398 [19 Jul 93] or higher DoD authority.
AUTHORITY
DTRA ltr, 1 Aug 2001

THIS PAGE IS UNCLASSIFIED

#627



**Defense Nuclear Agency
Alexandria, VA 22310-3398**



DNA-TR-93-84

Acoustic Resonance Spectroscopy in CW Verification Tooele Field Trial (August 1992)

**Dipen N. Sinha
Electronic Materials and Device Research Group
MS D429
Los Alamos National Laboratory
Los Alamos, NM 87545**

November 1993

Technical Report

CONTRACT No. IACRO-90-887 and IACRO-92-882

**Further dissemination only as directed by the Defense
Nuclear Agency, 6801 Telegraph Road, Alexandria, VA
22310-3398, 19 July 1993, or higher DoD authority.**

19990604 163

DESTRUCTION NOTICE:

FOR CLASSIFIED documents, follow the procedures in DoD 5200.22-M, Industrial Security Manual, Section II-19.

FOR UNCLASSIFIED, limited documents, destroy by any method that will prevent disclosure of contents or reconstruction of the document.

Retention of this document by DoD contractors is authorized in accordance with DoD 5220.22-M, Industrial Security Manual.

PLEASE NOTIFY THE DEFENSE NUCLEAR AGENCY,
ATTN: CSTI, 6801 TELEGRAPH ROAD, ALEXANDRIA, VA
22310-3398, IF YOUR ADDRESS IS INCORRECT, IF YOU
WISH IT DELETED FROM THE DISTRIBUTION LIST, OR
IF THE ADDRESSEE IS NO LONGER EMPLOYED BY YOUR
ORGANIZATION.



DISTRIBUTION LIST UPDATE

This mailer is provided to enable DNA to maintain current distribution lists for reports. (We would appreciate your providing the requested information.)

- ☐ Add the individual listed to your distribution list.
- ☐ Delete the cited organization/individual.
- ☐ Change of address.

NOTE:

Please return the mailing label from the document so that any additions, changes, corrections or deletions can be made easily.

NAME: _____

ORGANIZATION: _____

OLD ADDRESS**CURRENT ADDRESS**

TELEPHONE NUMBER: () _____

DNA PUBLICATION NUMBER/TITLE**CHANGES/DELETIONS/ADDITIONS, etc.)**

(Attach Sheet if more Space is Required)

DNA OR OTHER GOVERNMENT CONTRACT NUMBER: _____

CERTIFICATION OF NEED-TO-KNOW BY GOVERNMENT SPONSOR (if other than DNA):

SPONSORING ORGANIZATION: _____

CONTRACTING OFFICER OR REPRESENTATIVE: _____

SIGNATURE: _____

CUT HERE AND RETURN



REPORT DOCUMENTATION PAGE			Form Approved OMB No. 0704-0188	
Public reporting burden for this collection of information is estimated to average 1 hour per response including the time for reviewing instructions, searching existing data sources, gathering and maintaining the data needed, and completing and reviewing the collection of information. Send comments regarding this burden estimate or any other aspect of this collection of information, including suggestions for reducing this burden, to Washington Headquarters Services, Directorate for Information Operations and Reports, 1215 Jefferson Davis Highway, Suite 1204, Arlington, VA 22202-4302, and to the Office of Management and Budget, Paperwork Reduction Project (0704-0188), Washington, DC 20503				
1. AGENCY USE ONLY (Leave blank)	2. REPORT DATE 931101	3. REPORT TYPE AND DATES COVERED Technical 920401 - 930430		
4. TITLE AND SUBTITLE Acoustic Resonance Spectroscopy in CW Verification Tooele Field Trial (August 1992)		5. FUNDING NUMBERS C - IACRO-90-887 - IACRO-92-882		
6. AUTHOR(S) Dr. Dipen N. Sinha				
7. PERFORMING ORGANIZATION NAME(S) AND ADDRESS(ES) Electronic Materials and Device Research Group MS D429 Los Alamos National Laboratory Los Alamos, NM 87545		8. PERFORMING ORGANIZATION REPORT NUMBER LA-UR-93-1520		
9. SPONSORING/MONITORING AGENCY NAME(S) AND ADDRESS(ES) Defense Nuclear Agency 6801 Telegraph Road Alexandria, VA 22310-3398 OPAC/Johnston		10. SPONSORING/MONITORING AGENCY REPORT NUMBER DNA-TR-93-84		
11. SUPPLEMENTARY NOTES				
12a. DISTRIBUTION/AVAILABILITY STATEMENT Further dissemination only as directed by the Defense Nuclear Agency, 6801, Telegraph Road, Alexandria, VA 22310-3398, 19 July 1993, or higher DoD authority.			12b. DISTRIBUTION CODE	
13. ABSTRACT (Maximum 200 words) This report describes the Acoustic Resonance Spectroscopy (ARS) technique and details the various aspects of the NDE field trials carried out during August 1992 at the Tooele Army Depot in Utah. Test results for approximately 750 items including both conventional and chemical munitions are presented. The report also identifies various software and hardware modifications necessary to enhance the capabilities of the ARS system.				
14. SUBJECT TERMS Acoustic Technology Non-Destructive Evaluation Treaty Verification Technology Acoustic Resonance Spectroscopy			15. NUMBER OF PAGES 56	
			16. PRICE CODE	
17. SECURITY CLASSIFICATION OF REPORT UNCLASSIFIED	18. SECURITY CLASSIFICATION OF THIS PAGE UNCLASSIFIED	19. SECURITY CLASSIFICATION OF ABSTRACT UNCLASSIFIED	20. LIMITATION OF ABSTRACT SAR	

UNCLASSIFIED

SECURITY CLASSIFICATION OF THIS PAGE

CLASSIFIED BY:

N/A since Unclassified.

DECLASSIFY ON:

N/A since Unclassified.

SECURITY CLASSIFICATION OF THIS PAGE

UNCLASSIFIED

SUMMARY

This report details the various aspects of field trials carried out with the Acoustic Resonance Spectroscopy (ARS) systems developed by Los Alamos National Laboratory (LANL) during August 1992 at the Tooele Army Depot in Utah. Two portable ARS systems were used for the field trial exercise. One of the systems was used by a team of two inspectors from the On Site Inspection Agency (OSIA), and the other system by the LANL team, which consisted of two people.

The OSIA and LANL teams tested approximately 750 individual munition items, including both conventional and chemical munitions, as well as surrogate-filled munitions. ARS measurements were made on 105-mm (GB), 155-mm (GB, VX, H, WP, TNT, HE, ICM) rounds, 1-ton containers (GB and H), spray tanks, and MC-1 (GB) bombs. The identification of all 155-mm munition fill-types tested was highly successful. The ICMs showed unique acoustic signature. GB and mustard-filled 1-ton containers could be discriminated regardless of their fill level variations. Different types of algorithms were used for the 155-mm rounds and the bulk storage containers. Some difficulties were encountered in a few cases in which the data looked abnormal, but there was no way to verify the physical state of the munitions contents. The field tests were extremely valuable, both from the standpoint of the equipment tested and of the data gathered. Various software (data-acquisition and algorithm) and hardware modifications were identified that would be necessary before this system could be fielded.

CONVERSION TABLE

Conversion factors for U. S. Customary to metric (SI) units of measurement

MULTIPLY $\xrightarrow{\hspace{1cm}}$ BY $\xrightarrow{\hspace{1cm}}$ TO GET
 TO GET $\xleftarrow{\hspace{1cm}}$ BY $\xleftarrow{\hspace{1cm}}$ DIVIDE

angstrom	1.000 000 X E -10	meters (m)
atmosphere (normal)	1.013 25 X E +2	kilo pascal (kPa)
bar	1.000 000 X E +2	kilo pascal (kPa)
barn	1.000 000 X E -28	meter ² (m ²)
British thermal unit (thermochemical)	1.054 350 X E +3	joule (J)
calorie (thermochemical)	4.184 000	joule (J)
cal (thermochemical)/cm ²	4.184 000 X E -2	mega joule/m ² (MJ/m ²)
curie	3.700 000 X E +1	*giga becquerel (GBq)
degree (angle)	1.745 329 X E -2	radian (rad)
degree Fahrenheit	$T_K = (T^{\circ}F + 459.67)/1.8$	degree kelvin (K)
electron volt	1.602 19 X E -19	joule (J)
erg	1.000 000 X E -7	joule (J)
erg/second	1.000 000 X E -7	watt (W)
foot	3.048 000 X E -1	meter (m)
foot-pound-force	1.355 818	joule (J)
gallon (U.S. liquid)	3.785 412 X E -3	meter ³ (m ³)
inch	2.540 000 X E -2	meter (m)
jerk	1.000 000 X E +9	joule (J)
joule/kilogram (J/kg) (radiation dose absorbed)	1.000 000	Gray (Gy)
kilotons	4.183	terajoules
kip (1000 lbf)	4.448 222 X E +3	newton (N)
kip/inch ² (ksi)	6.894 757 X E +3	kilo pascal (kPa)
ktap		newton-second/m ² (N-s/m ²)
	1.000 000 X E +2	
micron	1.000 000 X E -6	meter (m)
mil	2.540 000 X E -5	meter (m)
mile (international)	1.609 344 X E +3	meter (m)
ounce	2.834 952 X E -2	kilogram (kg)
pound-force (lbs avoirdupois)	4.448 222	newton (N)
pound-force inch	1.129 848 X E -1	newton/meter (N · m)
pound-force/inch	1.751 268 X E +2	newton-meter (N/m)
pound-force/foot ²	4.788 026 X E -2	kilo pascal (kPa)
pound-force/inch ² (psi)	6.894 757	kilo pascal (kPa)
pound-mass (lbm avoirdupois)	4.535 924 X E -1	kilogram (kg)
pound-mass-foot ² (moment of inertia)		kilogram-meter ² (kg-m ²)
	4.214 011 X E -2	
pound-mass-foot ³		kilogram/meter ³ (kg/m ³)
	1.601 846 X E +1	
rad (radiation dose absorbed)	1.000 000 X E -2	**Gray (Gy)
roentgen		coulomb/kilogram (C/kg)
	2.579 760 X E -4	
shake	1.000 000 X E -8	second (s)
slug	1.459 390 X E +1	kilogram (kg)
torr (mm Hg, 0° C)	1.333 22 X E -1	kilo pascal (kPa)

*The becquerel (Bq) is the SI unit of radioactivity; 1 Bq = 1 event/s.

**The Gray (Gy) is the SI unit of absorbed radiation.

TABLE OF CONTENTS

SECTION	PAGE
SUMMARY	iii
CONVERSION TABLE	iv
FIGURES	vi
1 INTRODUCTION	1
2 EQUIPMENT DESCRIPTION.....	2
3 MEASUREMENT PROCEDURE	4
4 MUNITIONS TESTED	6
5 ALGORITHM	8
5.1 Basic Concept of the Algorithm.....	8
5.2 Working Premises	9
5.3 Making a Template	9
5.4 Munition Identification using Cross-Correlation	10
6 TEST RESULTS	11
6.1 Data Anaylsis	14
6.2 Surrogates.....	16
6.3 Application Scenario	16
7 CONCLUSIONS AND RECOMMENDATIONS	18
8 RESULTS SUMMARY	19
APPENDIX	
A Correlation Algorithm Results	21
B Template Frequency Data	25
C Modifications Required to Make ARS System Fieldable	27

FIGURES

Figure		Page
1	Acoustic Resonance Spectroscopy System	30
2	ARS Operation Selection Menu	31
3	General Information Input Screen	32
4	Graphical Display Screen During ARS Measurement	33
5	Graphical Representation of Template Generation Process	34
6	Comparability of Data Within a Given Class of Munitions	35
7	Comparision of Spectra Between Two Shell (munitions) Sizes	36
8	Comparison of Spectra Between H- and GB-Filled rounds	37
9	Comparison of Spectra Between VX- and GB-Filled Rounds	38
10	Comparison of 1-ton Container Spectra (Mustard and GB Fill)	39
11	Histogram of Data Shown in Figure 10	40
12	Comparison of Fourier Transform of 1-ton Container Spectra	41
13	Typical Spectra of GB-Filled MC-1 Bomb	42
14	Typical Spectra of HE-Filled 155-mm ICM	43
15	Typical Spectrum of VX Spray Tank (Effect of Weight)	44
16	Typical Spectrum of HE (solid)-Filled Rounds	45
17	Example of Abnormal Data	46
18	Comparison of Real (VX) vs. Surrogate-Filled Munitions	47
19	Comparison of Real (H) vs. Surrogate-Filled Munitions	48

SECTION 1

INTRODUCTION

Acoustic Resonance Spectroscopy (ARS), a nondestructive and noninvasive chemical weapons (CW) verification technique, has been under development at Los Alamos National Laboratory (LANL) for almost two years. This program has been funded by the Defense Nuclear Agency since April 1991. During August 19-26, 1992, the ARS instrumentation underwent field trial at the Tooele Army Depot in Utah. Two portable ARS systems were used for the field trial exercise. One system was used by a team of two inspectors from the On-Site Inspection Agency (OSIA) and the other by the LANL team of two physicists (Dr. Dipen N. Sinha and Dr. Kendall Springer). This report provides details of the ARS instrument used for the field trial, the test results, the algorithms used for data analysis, and the conclusions.

The main objectives of this field trial were to determine (1) the present status of the technology; (2) the suitability of the equipment for field use; (3) the reliability of the system when operated by personnel other than the scientists who developed the technology such as, inspectors from OSIA; and (4) the need for hardware, analysis algorithm, and user interface improvements.

SECTION 2

EQUIPMENT DESCRIPTION

The Acoustic Resonance Spectroscopy (ARS) system consists of three primary components: (1) DSA200 Digital Synthesizer and Analyzer unit, (2) Notebook computer, and (3) Transducer fixture (see Figure 1). The heart of the ARS system is the DSA200 unit (NEEL Electronics, CA) which is a rectangular box, approximately the size of a regular Notebook computer, and that contains a circuit board and rechargeable batteries (gels sels). The weight of the DSA200 unit is approximately 6 lbs, including battery. The battery lifetime for continuous operation varies between 6 and 8 hours, depending on the operating conditions and the unit can be fully charged in less than 4 hours. The battery life can be considerably improved by using rechargeable zinc-air batteries when they become available in a few months. The DSA200 unit included all electronic circuitry for carrying out sweep-frequency ARS measurements. It provided sine-wave excitation signal over a frequency range between 500 Hz and 100 kHz at selectable voltage levels from 10 mV to 10 V rms. Typical measurements used a frequency range between 1 and 30 kHz and an excitation voltage of <1 V rms. The DSA 200 unit also processed the received resonance signal and output it to the computer for real-time display and analysis.

We used two separate ARS systems for the field tests. One system was independently operated by the two OSIA inspectors and the other by the LANL team. The Notebook computer used by the OSIA team was a Zenith Z-NOTE 325L (a 386SX-25 MHz machine) while the LANL system used a Gateway 2000 486DX Notebook computer. Both of these systems could be operated using internal long life nickel metal hydride (NiMH) rechargeable batteries. We were able to carry out the entire day's assignments with a fully charged system. At the end of the day, both the DSA200 unit and the Notebook computers were recharged from 110 VAC outlets. The graphics display screens on both computers were monochrome LCD with VGA resolution and 32 gray scales. These computers were chosen specifically for their superior display quality, which did not wash out in bright and direct sunlight.

The transducer fixture consisted of an aluminum holder, two 1/2-inch diameter piezoelectric transducers (Panametrics Model V103 Videoscanner 1 MHz center frequency), and one voltage amplifier (NEEL Electronics RMT200). The transducers were held with metal rings inside a Teflon ribbon with two holes. The transducers were approximately 1 inch apart. The Teflon ribbon was attached to the aluminum holder, and it provided flexibility for transducer alignment on munition surface. Disc-shaped 1/2-inch diameter Neodymium-Iron-Boron magnets (Edmund Scientific) were firmly attached on the front face of the piezoelectric transducers and provided easy coupling between the transducers and the item being tested. The transducer fixture was connected to the DSA200 unit with a 30-foot long electrical cable. The maximum length of the cable could be as much as 100 feet. One of the transducers was used as a transmitter to excite vibrations on the item being tested while the second transducer detected the minute resonant vibrations that resulted. The typical drive signal for the transmitter was only 0.5 V, and the detected resonant vibration signal was less than 200 mV (following amplification) and corresponded to vibration amplitudes of the order of 100 angstroms. The excitation power was less than 1 mW and was distributed over the entire munition being tested; it never localized at a given spot. The total weight of the entire ARS system is approximately 12 lbs, including batteries. The equipment is portable and, although not specifically designed for field use, reasonably rugged. In fact, the OSIA system survived a several foot drop to the ground and functioned normally after that.

We also provided a miniature video (Private Eye) display that can be worn on the head over a mask. This display was specifically designed for situations where bright sunlight affected the readability of the computer. During our tests at Tooele, we never encountered a situation where we actually needed to use this miniature video display unit because the computer displays were quite adequate, even in bright sunlight. For a portable system, that is specifically designed for one-man operation of the ARS system, this miniature display could prove to be very convenient.

The DSA200 system contains all the necessary electronics and computer hardware for carrying out the frequency sweep measurements. The Notebook computer provides the supervisory control functions and an analysis of the data, including data storage and a graphics display. Typical sweep time used for most of the tests was 25 seconds. When the data analysis algorithms are optimized, this sweep (measurement) time can be reduced to 15 seconds depending on the munition type needed to be tested.

SECTION 3

MEASUREMENT PROCEDURE

In this section, we describe the actual measurement procedure using the ARS system. Most of the data-acquisition and analysis software were menu-driven for ease of operation. The software was written specifically so that a person with minimal training (less than 2 hours) would be capable of operating the equipment. Most of the operations could be carried out by pressing a single key. This single key control was found to be particularly useful because the operator needed to wear gloves during tests on chemical agent-filled munitions, which made normal typing on a computer keyboard rather difficult.

The first step was to make sure all the cables were connected properly. The Notebook computer communicates with the DSA200 unit through an RS232 cable. The transducer holder is connected to the DSA200 unit using a 30-foot-long cable. The computer and the DSA200 unit require a 2-minute warm-up. On power-up, the computer display comes up with a menu, as shown in Figure 2. This menu allows the selection of various ARS operations and automatically highlights the selection that needs to be executed in a sequence. Before taking any measurements on a munition item, the operator is required to enter some general information, which is then stored in the computer in an information file. Figure 3 shows the display on the computer screen for general information input. The name of the information file produced, following input to this screen, gets attached to each data set when actual ARS measurements are taken on munitions, and it can be retrieved quickly during data analysis. After the general information is input, the operator is prompted to calibrate the ARS system. This calibration process is not absolutely necessary but is recommended when working with unknown munitions. One can skip this procedure and proceed with the routine measurements. The calibration is done to determine the appropriate transducer excitation level for a given type of munition. This procedure needs to be carried out only once for any given class of munitions. It involves carrying out the sweep measurements a few times on a single item and adjusting the transducer drive level through computer input until the average signal level (acoustic spectrum) appears to be within a certain window. Future systems will have automatic calibration procedures.

The next process is to develop a template for a given class of munition (e.g., GB-filled 155-mm artillery shells). To develop a template, the operator simply selects five to ten items (the more the better) of the same kind and takes ARS measurements. Once the measurements are completed, the software automatically takes all of the data into consideration and generates the template information data file using the algorithm described in Section 5. We would like to point out that it is entirely possible to first take all the data from a large number of munitions and classify them according to agent type, etc. In that case, a template can be generated afterward.

The process for taking normal data is identical to the process of taking template data. In fact, one can take measurements on a large number of munition items of a given type, then, at a later stage, select a small group from the complete set to develop the template. Figure 4 is a copy of the actual computer display screen during measurement. The screen shows the operator all of the relevant information. All of the measurement parameters are displayed on the right side of the screen and can be edited by the operator. A running counter on the top-left corner of the screen displays the number of items tested. The status region at the bottom displays the results of the correlation, with a template (if one is available) for each measurement. The list of buttons at the bottom correspond to the

function keys on the computer keyboard. By pressing the appropriate function keys the operator can save the data acquired with automatic datafile naming and numbering, can rescale display, and can abort a sweep.

Following each process selected from the menu the display returns to the main menu. Instead of taking measurements, the operator can also choose to simply display previously stored data. In this data display mode, the operator can overlay data from different munition types for comparison.

SECTION 4

MUNITIONS TESTED

The following is a list of munitions tested by both the LANL and the OSIA teams during the period between August 19 and August 26, 1992. The parenthetical notations of "property" and "nuclear" in items 16 through 21 refer to surrogate liquids matched for physical property and elemental characteristics for nuclear experiments, respectively.

<i>Index</i>	<i>Munition Type</i>	<i>Number Tested</i>	
		<i>LANL</i>	<i>OSIA</i>
1	105-mm GB	17	34
2	1-ton GB	24	25
3	155-mm GB (Low Purity)	14	8
4	155-mm GB (High Purity)	13	15
5	MC-1 bomb GB	25	43
6	1-ton mustard	32	26
7	155-mm mustard	17	22
8	155-mm HE M483A1 (ICM)	20	14
9	M107 HE	29	16
10	155-mm VX	15	29
11	155-mm WP	31	30
12	8-inch VX	16	8
13	M106 TNT	17	6
14	Spray tank VX+empty	24	26
15	155-mm empty	8	
16	155-mm surrogate GB(property)	15	
17	155-mm surrogate H (property)	17	
18	155-mm surrogate VX(property)	17	
19	155-mm surrogate GB(nuclear)	15	
20	155-mm surrogate H (nuclear)	15	

<i>Index</i>	<i>Munition Type</i>	<i>Number Tested</i>	
		<i>LANL</i>	<i>OSIA</i>
21	155-mm surrogate VX(nuclear)	15	
22	155-mm surrogate sand	8	
23	1-ton surrogate	22	
<i>Total Number of measurements:</i>		426	302

The numbers on the two right-hand columns indicate the number of measurements made. In some cases, multiple measurements were made on the same item, particularly on the surrogate items. In most cases, however, the number of measurements correspond directly to the number of munitions tested.

SECTION 5

ALGORITHM

The correlation results (using *all* data sets) for eight classes of 155-mm munitions are presented in Appendix A. We are unable to provide statistically meaningful confidence levels to our measurements at this stage. We would like to point out that Appendix A contains *all* of the data sets, not just the specially selected ones. This analysis does not include fill-level variation correction and correction for weight when pallets are piled on top of each other (in some cases there were three levels of pallets on top). These corrections will further improve our analysis, but they will take time to implement. Even without the necessary corrections and refinements, the results presented in Appendix A are quite encouraging. Please see the section on Preliminary Data Analysis for more details.

With the ARS technique, an acoustic signature of a CW item is obtained by using the frequency sweep measurement and the essential features of that signature is compared with those from the known template signatures of various classes of munitions to determine which of the template signatures the unknown signature best correlates with. It was in this mode that the instrument was used in Tooele. Our goal was to determine whether one could classify CW munitions by their acoustic signatures. We accomplished this goal by first developing template signatures for various classes of munitions. We then used these templates as the reference signatures and compared them with the data sets from all classes. The results of this comparison are tabulated in terms of the degree of matching (quality of correlation) of all data sets with the templates from different classes. We found that the highest degree of correlation was indeed obtained between the munitions of a given class with the template of that class. Alternatively, the data from the different classes of munitions could be pooled and sorted according to type, based on their unique acoustic signature properties. In Section 5.1, we describe the method behind the algorithm we used.

The essential features of an acoustic signature consists of three parameters: (i) the resonance frequencies over a certain range, (ii) the peak amplitudes corresponding to the resonance frequencies, and (iii) the sharpness Q (Q is the ratio of the center frequency to the width of the resonance curve) of the resonance curves. We found that for artillery shells, such as 155-mm, 105-mm, M107 rounds etc., we could successfully classify the munition category (in this case, same shell type but containing different agent types) by using the resonance frequency information only. For robustness, however, one could use all three of the parameters listed above. For 1-ton containers, we used a slightly different, and simpler, approach. We found that the resonance Q s and the number of peaks are very different for mustard- and GB- filled containers. Simply by counting the peaks that exceed a certain threshold amplitude value, the two sets of data could be separately clustered. We discuss the algorithm used for the classification of artillery shells (e.g., 105-mm, 155-mm etc.) in greater detail below.

5.1 BASIC CONCEPT OF THE ALGORITHM.

Find the best match (highest correlation) of a set of resonant frequencies of unknown munitions with those of reference *templates* (known munitions).

5.2 WORKING PREMISES.

- A given munition item (e.g., artillery shell) possesses a set of *well-defined* and *reproducible* resonant frequencies (acoustic spectrum).
- A *subset* of these resonant frequencies can be excited and detected, depending on the manner in which the excitation is impressed upon the munition item (e.g., number of transducers, spacing between transducers, transducer placement, type of transducer etc.).
- Munition items with the same kind of shell type and fill type have *nominally identical* sets of resonant frequencies, but they can have small variations, on a finer scale, that depend on the condition of the munition.

5.3 MAKING A TEMPLATE.

A template is required to generate a reference signature of a certain category of munition. Data from an unknown munition is then compared (correlated) against a whole set of such templates and the best match is picked. The following steps describe the procedure used in generating a CW munition signature template. The process is shown graphically in Figure 5.

1. Acquire ARS data sets on N identical (size, shell type, fill type, etc.,) munition items.
2. Identify resonant peaks (frequencies) above a threshold amplitude (noise) value for each data set, and compile them into a single template file, that is, the number of data sets with resonance at frequency f , vs. f in the form of a barcode (Figures 5(a), 5(b), and 5(c)).
3. Replace each cluster of closely spaced peaks with a single, centrally weighted peak (see Figure 5(d), upper frame) using the following procedures:
 - i. Choose the frequency window width to allow for the expected frequency variation (e.g., variations due to tolerance variation and different fill levels, temperatures, loadings, etc.,) in individual peak frequencies among the data sets (munition items).
 - ii. Slide the window along the frequency axis. When the number-of-peak count within the window at any given position exceeds a threshold count (a certain percentage of N), that count value is assigned to the centroid (center of mass) frequency (calculated with respect to count distribution within the window).

Note: Template is not corrupted by inclusion of an accidental bad data set because a minimum (threshold) number of data sets must have a peak within the frequency window. Consequently, random isolated peaks have no effect on template generation. The window width is selected on the basis of a trade off between normal frequency variation, accommodation and sensitivity of discrimination. Appendix B provides a listing of the frequencies in the templates for eight different munition types generated using the above procedure.

5.4 MUNITION IDENTIFICATION USING CROSS-CORRELATION.

Determine peak positions (above a noise threshold) in the acoustic spectrum of an unknown munition item.

Cross-correlate the above peak positions (unknown data set) with the template data derived from multiple munitions (reference data).

Simple Correlation Equation:

$$Corr_u = \frac{100}{N_{ave}} \sum_{i=1}^{N_t} \sum_{j=1}^{N_u} \left(-\{sgn(f_i - f_u - \delta f) - sgn(f_i - f_u + \delta f)\} / 2 \right).$$

In the above equation, the subscripts **t** and **u** refer to template and unknown, respectively.

N_t, N_u: Number of frequency peaks in template and unknown datasets.

δf: The frequency windows used in correlation. It depends on the tolerances involved.

N_{ave}: The average number of resonance peaks in the template and the unknown datasets.

sgn: The mathematical sign function; it can take values of '+' and '-' depending on the sign of the argument within parentheses.

The above mathematical cross-correlation process provides the following information:

1. Total number of peaks that are common (within a predefined frequency spread-frequency window) to both template and unknown.
2. Determines which class the unknown item falls into. This process is done by cross-correlating the unknown data set with all the known templates. The template that produces the highest number determines the class for the unknown item. For a completely unknown munition (i.e., when no reference template is available for that class), the highest cross-correlation number gives an idea of the best possible match, even if it is not the correct match. Similarly, the second highest number provides a measure of the second best guess, and so on.

SECTION 6.

TEST RESULTS

In showing examples of typical acoustic spectra (raw data) for the various types of munitions that we tested, we have not included every type of munition tested, but only the ones we thought would be of interest. We remind the reader not to use this raw information for comparing every wiggle in the graphs among various munition types. A proper analysis of this raw data involves examining various parameters of the spectra, not simply comparing wiggles. Important parameters are the sharpness (Q) of the spectral lines; subtle frequency shifts in the right places (frequencies) where the liquid-shell coupling is the greatest; amplitude trend at higher frequencies; characteristics of the fundamental modes; high-frequency content, which may appear as noisy signal to the untrained eye; frequency dependent frequency shift; random frequency shift, etc. By considering all of these parameters, we can account for fill level variation and for the effect of loading, such as pallets on top of pallets etc., on the spectra. The simple algorithm described above does not take into account most of these parameters and, thus, underestimates the true potential of the ARS technique.

Figure 6 shows the comparability of the data within a given class. This figure shows an overlay of several data sets for 155-mm mustard-filled rounds. Important to note are the actual frequencies, and not the amplitudes or the nature of the shape. Eight munition data sets were selected randomly in this case, without paying any attention to whether or not the munitions were tested under identical conditions, such as similar pallet loading, etc. This provides a kind of worst-case scenario. As can be seen, the spectra are quite repeatable.

Figure 7 presents a comparison of the spectra from two different shell casings (8-inch and 155-mm) but with the same fill type GB. The difference in the spectra is obvious to the eye.

Figure 8 compares the spectra of 155-mm mustard (H) with 155-mm GB. Note the large difference in the Q (sharpness) values for an individual peak: 34 for H, as compared with 268 for GB. The average $\langle Q \rangle$ values are slightly different from these figures. Heavier and thicker liquids produce higher damping (lower Q) than lighter liquids such as GB. Q depends on a combination of factors such as viscosity, density, and, to some extent, the speed of sound. Also note how the H-data gradually damps out at higher frequencies. Another distinguishing characteristic is the obvious frequency shift to higher frequency for the lighter fluid.

Figure 9 presents a comparison between 155-mm VX and GB. The average $\langle Q \rangle$ values show a difference, 158 for VX as compared to 221 for GB. The GB in this case is the high purity GB. The frequency shifts are also quite obvious. This frequency shift, based on limited sampling, appears to be much larger than the variability observed within a given class. Again, the differentiation algorithm can take into account various other factors besides the simple frequency shift.

Figure 10 shows a comparison between 1-ton mustard and 1-ton GB data. The data in this case were taken by attaching the transducer head to the circular part of the container at the end and not on the cylindrical part of the container. Since the containers are stacked on top of each other, there is not sufficient access to the cylindrical side of the containers. In this case, we are primarily observing the excitations of the circular *drum*-

head of the container, which is primarily influenced by the fluid pressing against it and not due to the neighboring containers stacked against the cylindrical side. Consequently, the resonance characteristics are very different from those of the 155-mm rounds. Following our earlier discussion, it is worth pointing out that the GB data show a higher frequency content (noisier data by naked eye) as compared with the H data. This is another example of the effect of damping by the liquid. The heavier H damps out a lot of the vibrational modes of the front curved (circular) face where the measurements are made. This noisiness can be used as an effective discrimination parameter. One expedient method of quantifying the noisiness of the spectra is to simply count the total number of peaks above a certain threshold amplitude value.

Figure 11 shows the resonance peak count data for both H and GB in a histogram form. All data sets (see Table 1) are included in this histogram. As expected, the H data are all clustered on the left side of the plot and separated from the GB cluster on the right. This allows for a quick discrimination of the two types of munitions tested. There are various reasons for the large spread observed for the GB data. For example, the GB containers were stacked four levels as compared to only two levels for the H. The large pressure on the very bottom containers may have resulted in a damping effect on the vibrational characteristics of the circular front face and, thus, produced a somewhat lower count. There also could be some variation in fill level among all the containers: an emptier container would produce higher count. A somewhat more robust algorithm should be able to account for such variations. All of these deficiencies notwithstanding, we were able to achieve 100 percent correct classification, as shown below. These results of the 1-ton container data are summarized below. Measurements from both the LANL and OSIA teams are presented. The confidence levels were derived from simple Binomial statistics, which significantly underestimates the true value. At present, we do not have a better method for estimating a confidence level because of the simple algorithm we used. A second analysis approach was to examine the FFT (Fast Fourier Transform) of the spectra, as shown in Figure 12. The noisier GB data show large high-frequency components, as expected, compared with that of the H data. Also the average value of the FFT amplitude is significantly higher for GB than for H, as shown by the horizontal line. It should be pointed out that the template matching technique, in its present form, is not useful for the bulk storage containers. A lot more modeling effort would be needed to develop a robust algorithm for the bulk containers. For the present, the ad hoc methods presented here seem to be quite effective.

Table 1. 1-ton container results.

Team	Agent Type	Number of Incorrect Categorizations	Number of Samples (Tested)	90% Lower Confidence	95% Lower Confidence
LANL	Mustard	0	32	93	91
	GB	0	24	91	88
OSIA	Mustard	0	26	90	89
	GB	0	21	89	87

Figure 13 shows typical data from MC-1 bombs. Most data within the class show good repeatability. Again, the data analysis here is very similar to that of the 1-ton containers. For comparison, we have presented the data taken from the Lakeside bomb. A simple examination of this data, by eye, indicates two possible explanations for the large shift in the data toward lower frequency for the Lakeside bomb. It indicates that there might

be some water inside and, most likely, that the shell has thickened and weakened (become less stiff) due to extensive rusting. Similar to the case of 1-ton containers, the algorithm developed for 105-mm and 155-mm shells may not be directly applicable to the MC-1 bombs. The present algorithm would have to be refined further.

Figure 14 presents an interesting case of the 155-mm HE ICM (Improved Conventional Munition) munitions that contain grenades. The characteristics of this data are very different from those of simple HE-filled munitions, such as Comp-B and TNT, that have no burster core. The sharp peaks identified by arrows correspond to the circumferential vibration modes. The frequency separation f between consecutive peaks show a gradual increase because the top part of the shell is tapered (conical) and, thus, has a gradually smaller circumference as it approaches the top. After proper processing of the data, it may be possible to identify munitions such as ICMs. Our preliminary modeling of ICMs indicate that grenades also resonate inside along the axis of the shell. The peaks between 5 and 10 kHz include the grenade resonances as well as the shell modes.

An example of spray tank data is shown in Figure 15. In this case, the measurements were made on the outside container of the spray tank to see if it was possible to determine, without opening the container, whether a spray tank container contains an empty tank (or no tank). The principle behind this is that a fully loaded spray tank will stress the struts in the container differently than will an empty tank. The effect of this stress should show up as frequency shifts. Consequently, we have taken data on both loaded and unloaded containers. The data shown suggest that it may be possible to determine the container loading effect, as mentioned above, but the present data are insufficient to allow any definitive claims to be made at this stage. We feel it is worthwhile to pursue this approach more systematically.

In Figure 16, we show typical characteristics of HE (solid)-filled rounds. Both M107 and 155-mm rounds have lower vibrational modes (usually corresponding to the bending modes of the shell casing) that lie between 2 and 5 kHz. These modes are strongly affected only by the weight of the fill material inside, and they are somewhat immune to the quality of the contact between the fill and the inside wall of the shell casing. In the case of the HE-filled rounds, these lower modes also show low Q-values and low amplitudes. In addition, the average amplitude above 10 kHz is also very low for the HE-filled rounds, in comparison with the liquid-filled rounds. Our present algorithm does not incorporate these features into the analysis of the data. It may, however, be possible to do so if we further refine our algorithm to discriminate between solid and liquid fill types without using a template but simply by examining certain features in the spectrum. However, to accomplish this will require both modeling and experimental studies.

Figure 17 shows a typical example of bad (abnormal) data. We found a few cases like this, which did not correlate with any templates. The high-frequency components are heavily damped, and the peaks are below the threshold amplitude value used in our algorithm. Our best guess is that the GB in this round has somehow gelled or solidified. We have no way to verify this and will never know the reasons. Without knowing the actual physical state of the fill, it is difficult to explain the spectrum. However, with better A/D resolution and a front-end logarithmic amplifier in our ARS electronics, it may be possible to extract meaningful information, even from such abnormal data sets, and to correlate with known templates.

Finally, we would like to point out that we were able to take data on 155-mm shells that were in the interior of the palette. This was possible because the probe (transducer fixture) used was quite small and could be inserted through the space available near the neck of the munition shells. This probe size can be reduced further without affecting the

sensitivity of the measurements. All measurements were made without moving the munitions.

6.1 DATA ANALYSIS.

The attached listing (see Appendix A) shows the results of our correlation algorithm for determining whether a munition belongs within a class and for differentiating among munitions from different classes (liquids such as H, VX, GB etc.). The algorithm first establishes a baseline information template from data taken from known classes of munitions. This template then includes all the variability in the spectra that one observes in the data from real munitions. Once templates for various munitions are established, the acoustic resonance spectrum from any unknown munition can then be cross-correlated with this template quickly. In this listing, we have taken all the data files (corresponding to all 155-mm munitions) from our measurements and run them through this algorithm to see how well the unknown raw data correlated with the known templates. At this time, we cannot provide any quantitative confidence level to the results, except by using a simple binomial statistics approach, which seriously underestimates the true confidence level. The listing provides the best match (first), the second best match, and the third best match from the known templates. In a few instances, there were ties between the best and the second best correlations. These instances were resolved by including secondary information, such as correlation value obtained with twice the frequency bin width. In our correlation algorithm, the correlation value was always calculated for a selected fixed bin width and also for twice the bin-width. In most situations, where the correlation values for the best and the second best correlations were clearly demarcated, the additional information was not used.

A completely unknown munition will pick out the munition type it matches most closely from the known templates. This algorithm can be significantly refined and can be made more robust if proper correction factors for fill-level variations and weight on top of munitions (e.g., pallets on top of pallets) are taken into account. This robustness can be further improved by including the Q-factors in the correlation algorithm. Q-factor calculations require good peak location algorithms. The peak location algorithm used for the present analysis was adequate, but we have since refined it further. However, no new data analyses were carried out with the improved peak location and Q-determination algorithms.

In Table 2, we show the GB data in two different ways. The LANL data were tested with a sharper discrimination (frequency) window that enabled the distinction between low and high purity GB. It is a simple matter to widen the discrimination window and only retain the ability to discriminate GB from other agents. This was done with the OSIA data as an example. In other words, making the ARS discrimination less sensitive for broader classification capabilities is simple, although, it does have the ability of much finer discrimination. It should be pointed out that, to avoid possible errors, the data-acquisition parameters (e.g., number of points, frequency range, frequency steps, and sweep rate) should be kept the same for data taken for templates and during normal measurements on unknown munitions. With a further refinement in the algorithm, this restriction can be lifted.

Table 2. 155-mm round data.

155-mm	LANL DATA		OSIA DATA	
Agent Type	Number of Incorrect Categorizations	Number of Samples	Number of Incorrect Categorizations	Number of Samples
GB (High Purity)	0	13	0	20
GB (Low Purity)	0	13		Includes both Low and High
Mustard	0	16	2	17
VX	0	15	1	14
White Phosphorus	0	23		
TNT	0	15		

Note: The OSIA results include data that were incorrectly measured, such as saturated peaks (*amplifier saturation*), and that make it difficult to identify peaks. Nevertheless, the correct identifications were the second choice. With refined algorithm the identification process can be made more robust.

In Table 3 we summarize the data from various 155-mm shells and combine the data taken by the LANL and OSIA team. We have also discarded the known bad data sets (as described above) from the OSIA data list.

Table 3. Combined LANL and OSIA data for 155-mm rounds.

Agent Type	Number of Incorrect Categorization	Number of Samples (Tested)	90% Lower Confidence	95% Lower Confidence
Mustard	0	31	93	91
GB	0	46	95	93
VX	0	28	92	90
TNT	0	15	86	82
White Phosphorus	0	23	90	88

It is worth pointing out that the templates for each class of munition tested (specifically, the 155-mm rounds) are almost entirely interchangeable between the LANL and OSIA data. This is notwithstanding the fact that the OSIA team only took half as many

data points as the LANL team (1000 vs 2000). Consequently, the OSIA team acquired data twice as fast. Normally, the frequency sweep speed affects the measurement of sharp resonance Qs, but we found this effect to be minimal enough that it did not affect the final results. This gives us some confidence in the algorithm and the procedures adapted for the ARS measurement. We believe that with further refinement of the algorithm, a template reference library of various classes of munitions can be reliably generated even if the data are obtained from different sources and different people operating the equipment.

6.2 SURROGATES.

The data from the surrogates are classified as separate categories from the real agent-filled munitions by our algorithm. This implies that the property matched surrogates used do not represent the real munition. On close visual examination of the data, we found the reasons for this discrepancy. Figures 18 and 19, respectively, compare the VX and H surrogate data with the real munition data. In the VX data, the resonance Qs are reasonably matched, but the frequencies are way off. Figure 18 overlays multiple data sets to show that there is a systematic difference. In Figure 19, the mustard data shows that the resonance frequencies are reasonably close, but the resonance Qs are dramatically different. In the case of the mustard data, we do not know the real physical condition of the agent. It is possible that the agent has physically degraded and significantly thickened and that the shell wall-liquid interface properties are altered, to a large degree, from what could be expected from fresh agent. This effect cannot be reproduced by the surrogates. These are mere speculations since we do not have any direct knowledge of the exact state of the agent inside the rounds. On the face of the available information, we have to conclude that the physical property matched munitions do not represent the real ones from the ARS point of view. This also implies that the ARS technique is reasonably resistant to spoofing.

6.3 APPLICATION SCENARIO.

We feel that the particular strength of the ARS technique is in rapidly screening a large number of munitions to determine a given class. Because of the nature and the sensitivity of this technique, it can also be used for safety checks in munitions and for quality control. For instance, it may be possible to detect voids or detachment of contents, such as Comp-B, TNT etc., from the inside wall. We have not explored all the different possibilities. We do not want leave the impression that we can ever image the contents of munitions.

Our current test system is composed of two separate units. It is rather straightforward to combine both these units into one. The system can be operated by a single person, as it is designed, but a two-person operation in the field is recommended. The weight of the entire ARS system can be as little as 10 lbs, including batteries. For much longer continuous operation, however, an additional battery pack may be required, which will increase the weight by 2-4 lbs. This battery weight can be significantly reduced when the new high-efficiency zinc-air rechargeable batteries are available (second quarter 1993). The present system has the built-in design for wireless data communication between the DSA200 unit and the Notebook computer. For situations where some treaty-limited items need to be monitored for a long duration, such wireless communication may be desirable for remote monitoring. The power consumption of the DSA200 unit is low enough that it can be operated from a commercially available 1-foot-square solar cell power-generation unit.

The ARS system, in its present implementation, does not provide fill level information directly. However, such information can be extracted if the system is

calibrated against known fill levels. We are currently developing algorithms to derive universal fill-level calibration that can be used for given types (shape) of munitions, such as 105-mm, 155-mm, M106, M107 etc. All 1-ton containers, thus, can have a single calibration. For 55-gallon drums, the situation is slightly different. Because the metal skin of the drum is very thin, compared with the artillery shells and the 1-ton containers, it is possible to directly determine the fill level in such drums by moving the transducers on the outer surface of the drum vertically. The local mechanical vibrations damp out severely when there is liquid present on the other side. In this case the frequency sweep is done very fast because detailed resonance information is not required. The same magnetically attached transducers are used.

The ARS technique does not directly determine physical properties of chemical agents but primarily determines whether the acoustic spectra from a known baseline matches the spectrum from an unknown munition. For completely unknown munitions, however, it is still possible to determine the general nature of the fill, such as solid, liquid, or gel, without having known baseline information. From our modeling efforts, we feel that it may be possible to scale information from one size of munition to the other. This improvement will take time to develop and verify on real munitions.

SECTION 7

CONCLUSIONS AND RECOMMENDATIONS

We found the exercise at Tooele very useful. It provided us with a lot of important information we did not have before regarding the nature of the acoustic signature for different types of munitions. It was also very important to have the feedback from the OSIA inspectors regarding the operation of the system under realistic conditions. This will help us improve the system further. The extensive amount of data we were able to gather will help us significantly in refining our algorithms.

Based on our preliminary data analysis, we were able to differentiate between VX, GB, and mustard, and between solid and liquid fill. However, the solid and liquid discrimination used the same template correlation method and did not rely on any ad hoc process. We do not yet have a reliable algorithm that can discriminate between solid and liquid fill with 100 percent accuracy without using any baseline information, primarily because, in some solid-filled munitions, the fill material inside is detached from the inside wall of the munition. Although it is quite possible to use information, such as the damping of the fundamental modes, to discriminate between solid and liquid fill, regardless of fill detachment, the algorithm needs to be experimentally verified, and there is no current scope for doing that at present. The algorithm is based on the fact that the lower modes are primarily affected by the actual mass of the fill material in the first order. Developing this algorithm further might also require that the measurement approach be modified. For example, a higher level of excitation might be needed at the lower frequencies. We found the ARS technique to be sensitive enough to provide information beyond that mentioned in this report. Further research can improve the technique and make useful in other CW treaty verification areas as well.

We do not feel that the system is ready for field deployment yet; it will require a certain amount of hardware and software modifications (*see Appendix C for a complete listing of recommended hardware and software modifications*). Some of these modifications are straightforward and can be carried out in a relatively short period of time. The algorithms also need to be further refined to minimize false positives. Achieving the full potential of this technique will require at least one more year's worth of R&D effort. Based on the results so far, we are very optimistic that the system can be improved significantly so that it can become a truly reliable tool for chemical weapons treaty verification. Simple variations of the ARS technique can produce instruments that can be very useful in treaty verification. In particular, a very simple hand-held calculator-size system can be built that could, in less than 5 seconds, determine whether a munition is solid or liquid filled. Based on our laboratory studies, it appears to be possible to directly probe the chemical agent inside munitions and to receive information regarding both the chemical and the physical nature of the agent. The technique is another variation of the ARS technique. If this is realized, it may be possible to test unknown munitions without being affected by munition size, shape, or wall thickness. The development of this technique will require at least a year's worth of effort. We recommend that the ARS system should not be fielded without the improvements mentioned. We also recommend, however, that complementary techniques be used in conjunction with the ARS technique. For example, the ARS technique may be used for quick screening of munitions, whereas other techniques, such as PINS, can be used on a small sample to determine the chemical nature of the agent. For fill level measurement in bulk containers, UPE is currently a better solution.

SECTION 8.

RESULTS SUMMARY

- Same templates worked for both LANL and OSIA data, although each team used a different number of data points and widely different sweep rates. However, we do not recommend this approach of using data obtained using disparate measurement parameters for template correlation without further refinement in the algorithm.
- Measurement time, between 15-20 seconds, and 1000 or less data points in a data set seem acceptable but may be borderline for actual use. A typical data set can be ~2 kByte. This implies that approximately 60,000 measurements can be stored in a typical 120- MByte hard disk drive of a Notebook computer and 1,000 data sets in a high-density floppy diskette. If one uses the recently introduced DOS 6.0 (or equivalent) file compression techniques, this data storage capacity can be doubled without any hardware change.
- Majority of the munitions tested at Tooele produced good quality data, and the data were well behaved, as expected. A few bad cases were found, but there was no way to determine why they were bad without actually opening up the munition. There was no way to verify the nature of the contents.
- It was possible to discriminate between real munitions and surrogate-filled (physical property matched liquids) munitions. This indicates that the ARS technique is reasonably resistant to spoofing. Further studies are recommended.
- Contents (GB, H) of 1-ton containers could be discriminated regardless of fill level and other variations.
- ICMs have unique characteristics and can be easily discriminated.
- The results of the spray-tank container loading are inconclusive, but the method does show some promise and deserves further investigation.
- Determination of fill-level in bulk storage containers will require modeling and further analysis of the data.
- Besides identifying seven different fill types, this technique was successful in discriminating between high- and low-purity GB.
- Determination of physical properties (speed of sound, density, and viscosity) of chemical agents is possible with the ARS technique but will require further study.
- A simpler system (hand-held calculator size), adapted from the present ARS technique, can be built that can provide rapid (~2 second) discrimination between conventional (solid) and chemical or biological munitions.
- Configuration-dependent pattern in the acoustic signature could be identified from the data gathered at Tooele. It may be possible to use this information in scaling data from unknown munition types to match against known templates. This approach looks promising and deserves further study.

- The recent exercise at Tooele showed that the ARS technique can be fine tuned to determine the state of the agent fill, such as solidification, stratification, degradation etc., but would require systematic study before such features can be implemented.
- With further refinement of the algorithm and improved hardware (transducers and electronics) the ARS technique can be made very reliable. The Tooele tests helped identify several specific improvements that need to be made to the existing system before it can be fielded.

APPENDIX A

CORRELATION ALGORITHM RESULTS

Nomenclature:

The first column of the table below lists the filename of each munition tested. The munition type is encoded into the filename using a four-letter designation as described below. Example: GH550601 refers to 155-mm High Purity GB. The file extension ".bin" refers to the fact that the data are stored in binary form in the computer. The number of resonance peaks in each spectrum is also listed in the last column.

GH55: 155-mm High Purity GB	(GB-hi)
GL55: 155-mm Low Purity GB	(GB-low)
H055: 155-mm Mustard	(H)
VX55: 155-mm VX	(VX)
WP55: 155-mm White Phosphorous	(WP)
TNT6: M106 TNT	(TNT)
S55G: 155-mm Surrogate GB (Physical Property)	(GB-Sur)
S55H: 155-mm Surrogate H (Physical Property)	(H-Sur)
S55V: 155-mm Surrogate VX (Physical Property)	(VX-Sur)

Munition Data	Best Correlation	Second Best Correlation	Third Best Correlation	Number of Peaks used
GH550601.bin	1st: GB-hi	2nd: VX	3rd: H-Sur	(87)
GH550702.bin	1st: GB-hi	2nd: GB-low	3rd: GB-Sur	(73)
GH550503.bin	1st: GB-hi	2nd: GB-Sur	3rd: H-Sur	(58)
GH55XX04.bin	1st: GB-hi	2nd: GB-low	3rd: WP	(60)
GH550305.bin	1st: GB-hi	2nd: GB-low	3rd: H-Sur	(94)
GH550806.bin	1st: GB-hi	2nd: WP	3rd: GB-Sur	(68)
GH550107.bin	1st: GB-hi	2nd: GB-low	3rd: WP	(64)
GH550208.bin	1st: GB-hi	2nd: WP	3rd: GB-Sur	(54)
GH550a01.bin	1st: GB-hi	2nd: H-Sur	3rd: GB-low	(54)
GH550c02.bin	1st: GB-hi	2nd: GB-Sur	3rd: WP	(59)
GH550d03.bin	1st: GB-hi	2nd: WP	3rd: GB-low	(53)
GH550g04.bin	1st: GB-hi	2nd: GB-low	3rd: H-Sur	(82)
GH550n05.bin	1st: GB-hi	2nd: VX-Sur	3rd: WP	(75)
GL551301.bin	1st: GB-low	2nd: VX	3rd: GB-hi	(58)
GL551502.bin	1st: GB-low	2nd: VX	3rd: GB-hi	(80)
GL551603.bin	1st: GB-low	2nd: GB-hi	3rd: H	(52)
GL550904.bin	1st: GB-low	2nd: GB-hi	3rd: WP	(52)
GL551105.bin	1st: GB-low	2nd: WP	3rd: GB-hi	(36)
GL551006.bin	1st: GB-low	2nd: GB-hi	3rd: VX	(64)
GL551407.bin	1st: GB-low	2nd: WP	3rd: TNT	(50)
GL551208.bin	1st: GB-low	2nd: VX	3rd: TNT	(70)
GL550a09.bin	1st: GB-low	2nd: VX	3rd: GB-hi	(78)
GL559b10.bin	1st: GB-low	2nd: GB-hi	3rd: VX	(76)

GL550c11.bin	1st: VX-Sur	2nd: H-Sur	3rd: WP	(40)
GL550d01.bin	1st: GB-low	2nd: WP	3rd: VX	(55)
GL550e02.bin	1st: GB-low	2nd: WP	3rd: VX	(55)
GL550f03.bin	1st: GB-low	2nd: GB-hi	3rd: H-Sur	(67)
H0551001.bin	1st: H	2nd: WP	3rd: VX-Sur	(11)
H0551302.bin	1st: H	2nd: VX-Sur	3rd: H-Sur	(13)
H0551403.bin	1st: H	2nd: GB-Sur	3rd: H-Sur	(17)
H0551604.bin	1st: H	2nd: VX-Sur	3rd: GB-Sur	(13)
H0551505.bin	1st: H	2nd: H-Sur	3rd: WP	(16)
H0550406.bin	1st: H	2nd: TNT	3rd: H-Sur	(14)
H0550607.bin	1st: H	2nd: H-Sur	3rd: VX-Sur	(15)
H0550508.bin	1st: H	2nd: VX-Sur	3rd: H-Sur	(21)
H0550109.bin	1st: H	2nd: H-Sur	3rd: VX-Sur	(17)
H0551110.bin	1st: H	2nd: H-Sur	3rd: TNT	(12)
H0550211.bin	1st: H	2nd: VX-Sur	3rd: H-Sur	(13)
H0550312.bin	1st: H	2nd: H-Sur	3rd: VX-Sur	(12)
H0550813.bin	1st: H	2nd: VX-Sur	3rd: H-Sur	(15)
H0550914.bin	1st: H	2nd: VX-Sur	3rd: TNT	(12)
H0550716.bin	1st: H	2nd: H-Sur	3rd: VX-Sur	(11)
H0557c17.bin	1st: H	2nd: H-Sur	3rd: VX-Sur	(15)
VX551401.bin	1st: VX	2nd: GB-low	3rd: TNT	(67)
VX551302.bin	1st: VX	2nd: TNT	3rd: GB-low	(47)
VX551503.bin	1st: VX	2nd: GB-low	3rd: H	(68)
VX551104.bin	1st: VX	2nd: TNT	3rd: GB-hi	(48)
VX551005.bin	1st: VX	2nd: TNT	3rd: H	(64)
VX551206.bin	1st: VX	2nd: GB-low	3rd: VX-Sur	(57)
VX550907.bin	1st: VX	2nd: GB-low	3rd: GB-hi	(55)
VX550808.bin	1st: VX	2nd: GB-low	3rd: TNT	(53)
VX550709.bin	1st: VX	2nd: VX-Sur	3rd: TNT	(66)
VX550510.bin	1st: VX	2nd: TNT	3rd: GB-low	(57)
VX550411.bin	1st: VX	2nd: GB-low	3rd: GB-hi	(49)
VX550612.bin	1st: VX	2nd: H	3rd: GB-low	(60)
VX550313.bin	1st: VX	2nd: GB-low	3rd: VX-Sur	(67)
VX550214.bin	1st: VX	2nd: GB-hi	3rd: GB-low	(66)
VX550101.bin	1st: VX	2nd: TNT	3rd: VX-Sur	(53)
WP550401.bin	1st: WP	2nd: GB-low	3rd: TNT	(41)
WP550502.bin	1st: WP	2nd: GB-low	3rd: GB-Sur	(42)
WP55XX03.bin	1st: WP	2nd: TNT	3rd: VX-Sur	(33)
WP551504.bin	1st: WP	2nd: H	3rd: GB-low	(24)
WP550807.bin	1st: WP	2nd: GB-low	3rd: GB-hi	(37)
WP550708.bin	1st: WP	2nd: VX-Sur	3rd: GB-hi	(42)
WP550609.bin	1st: WP	2nd: H-Sur	3rd: GB-hi	(40)
WP551010.bin	1st: WP	2nd: GB-hi	3rd: GB-low	(45)
WP550911.bin	1st: WP	2nd: GB-Sur	3rd: H	(33)
WP551212.bin	1st: WP	2nd: GB-low	3rd: GB-hi	(30)
WP551313.bin	1st: WP	2nd: TNT	3rd: H	(15)
WP551314.bin	1st: WP	2nd: VX-Sur	3rd: TNT	(34)
WP551915.bin	1st: WP	2nd: GB-low	3rd: H	(40)
WP551816.bin	1st: WP	2nd: GB-low	3rd: VX	(36)
WP552017.bin	1st: WP	2nd: GB-hi	3rd: GB-Sur	(35)
WP551718.bin	1st: WP	2nd: H	3rd: GB-low	(42)
WP550019.bin	1st: WP	2nd: GB-hi	3rd: GB-Sur	(50)
WP550120.bin	1st: WP	2nd: GB-hi	3rd: GB-low	(40)
WP550221.bin	1st: WP	2nd: H	3rd: TNT	(34)

WP550a22.bin	1st: WP	2nd: VX	3rd: GB-hi (45)
WP550g01.bin	1st: WP	2nd: GB-hi	3rd: GB-low (34)
WP550h02.bin	1st: WP	2nd: GB-hi	3rd: H (5)
WP550i03.bin	1st: WP	2nd: GB-hi	3rd: GB-low (33)
TNT60101.bin	1st: TNT	2nd: WP	3rd: VX-Sur (46)
TNT60303.bin	1st: TNT	2nd: VX-Sur	3rd: GB-Sur (50)
TNT60404.bin	1st: TNT	2nd: VX-Sur	3rd: H-Sur (25)
TNT60505.bin	1st: TNT	2nd: VX-Sur	3rd: GB-Sur (45)
TNT60606.bin	1st: TNT	2nd: H-Sur	3rd: VX-Sur (34)
TNT60707.bin	1st: TNT	2nd: H-Sur	3rd: H (33)
TNT60808.bin	1st: TNT	2nd: VX-Sur	3rd: H-Sur (47)
TNT60909.bin	1st: TNT	2nd: VX-Sur	3rd: H (35)
TNT61010.bin	1st: TNT	2nd: VX-Sur	3rd: GB-Sur (45)
TNT61111.bin	1st: TNT	2nd: VX-Sur	3rd: H-Sur (38)
TNT61312.bin	1st: TNT	2nd: VX-Sur	3rd: H-Sur (44)
TNT61213.bin	1st: TNT	2nd: VX-Sur	3rd: H-Sur (41)
TNT61414.bin	1st: TNT	2nd: VX-Sur	3rd: GB-Sur (38)
TNT61615.bin	1st: TNT	2nd: VX-Sur	3rd: H-Sur (42)
TNT61516.bin	1st: TNT	2nd: WP	3rd: VX-Sur (47)
S55G0301.bin	1st: GB-Sur	2nd: VX-Sur	3rd: H-Sur (77)
S55G0302.bin	1st: GB-Sur	2nd: H-Sur	3rd: TNT (61)
S55G0403.bin	1st: GB-Sur	2nd: WP	3rd: VX-Sur (56)
S55G0404.bin	1st: GB-Sur	2nd: GB-low	3rd: GB-hi (65)
S55G0105.bin	1st: GB-Sur	2nd: GB-hi	3rd: WP (53)
S55G0106.bin	1st: GB-Sur	2nd: WP	3rd: GB-hi (49)
S55G0207.bin	1st: GB-Sur	2nd: H-Sur	3rd: H (50)
S55G0208.bin	1st: GB-Sur	2nd: H-Sur	3rd: H (53)
S55G0509.bin	1st: GB-Sur	2nd: GB-hi	3rd: VX-Sur (46)
S55G0510.bin	1st: GB-Sur	2nd: WP	3rd: H-Sur (55)
S55G0301.bin	1st: GB-Sur	2nd: TNT	3rd: H-Sur (82)
S55G0402.bin	1st: GB-Sur	2nd: GB-hi	3rd: VX (50)
S55G0103.bin	1st: GB-Sur	2nd: WP	3rd: GB-hi (50)
S55G0204.bin	1st: GB-Sur	2nd: H-Sur	3rd: VX-Sur (56)
S55G0505.bin	1st: GB-Sur	2nd: VX	3rd: H (49)
S55H0201.bin	1st: H-Sur	2nd: H	3rd: VX-Sur (54)
S55H0202.bin	1st: H-Sur	2nd: VX-Sur	3rd: H (58)
S55H0103.bin	1st: H-Sur	2nd: VX-Sur	3rd: GB-Sur (49)
S55H0305.bin	1st: H-Sur	2nd: VX-Sur	3rd: H (42)
S55H0306.bin	1st: H-Sur	2nd: VX-Sur	3rd: H (61)
S55H0507.bin	1st: H-Sur	2nd: VX-Sur	3rd: TNT (60)
S55HXX08.bin	1st: H-Sur	2nd: VX-Sur	3rd: H (63)
S55H0509.bin	1st: H-Sur	2nd: VX-Sur	3rd: H (70)
S55H0410.bin	1st: H-Sur	2nd: VX-Sur	3rd: H (47)
S55H0411.bin	1st: H-Sur	2nd: VX-Sur	3rd: H (53)
S55H0301.bin	1st: H-Sur	2nd: VX-Sur	3rd: H (37)
S55H0302.bin	1st: H-Sur	2nd: VX-Sur	3rd: H (76)
S55H0203.bin	1st: H-Sur	2nd: VX-Sur	3rd: GB-low (78)
S55H0104.bin	1st: H-Sur	2nd: GB-Sur	3rd: TNT (54)
S55H0405.bin	1st: H-Sur	2nd: VX-Sur	3rd: H (67)
S55H0506.bin	1st: H-Sur	2nd: VX-Sur	3rd: GB-low (62)
S55V0501.bin	1st: VX-Sur	2nd: H	3rd: TNT (46)
S55V0502.bin	1st: VX-Sur	2nd: H-Sur	3rd: GB-Sur (68)
S55V0503.bin	1st: VX-Sur	2nd: H-Sur	3rd: TNT (50)
S55V0204.bin	1st: VX-Sur	2nd: H	3rd: H-Sur (72)

S55V0405.bin	1st: VX-Sur	2nd: H-Sur	3rd: TNT	(51)
S55V0406.bin	1st: VX-Sur	2nd: H-Sur	3rd: TNT	(43)
S55V0307.bin	1st: VX-Sur	2nd: H-Sur	3rd: H	(55)
S55V0308.bin	1st: VX-Sur	2nd: H-Sur	3rd: TNT	(62)
S55V0109.bin	1st: H	2nd: VX-Sur	3rd: H-Sur	(48)
S55V0110.bin	1st: VX-Sur	2nd: H	3rd: H-Sur	(42)
S55V0511.bin	1st: VX-Sur	2nd: H	3rd: H-Sur	(66)
S55V0112.bin	1st: VX-Sur	2nd: H-Sur	3rd: H	(62)
S55V0501.bin	1st: VX-Sur	2nd: H-Sur	3rd: H	(45)
S55V0102.bin	1st: VX-Sur	2nd: H	3rd: H-Sur	(42)
S55V0303.bin	1st: VX-Sur	2nd: H-Sur	3rd: H	(48)
S55V0404.bin	1st: VX-Sur	2nd: H-Sur	3rd: TNT	(52)
S55V0205.bin	1st: VX-Sur	2nd: H-Sur	3rd: H	(46)

APPENDIX B

TEMPLATE FREQUENCY DATA

All data are for 155-mm munitions. The numbers in the table are frequencies in kilohertz. The following table is a simple list of peak frequencies in the template for each munition type. These data are extracted from the raw data of many items of each type. There is *no* row-by-row correspondence of numbers in this table (i.e., do *not* simply try to correlate these numbers by row).

Hgh-Purity GB	Low-Purity GB	Surrogate GB	H	Surrogate H	Surrogate VX	VX	WP	TNT
3.94	4	2.665	1.525	3.745	3.745	4.06	2.755	3.775
5.23	5.26	3.805	2.26	4.435	3.835	5.365	3.88	4.51
5.395	5.5	4.555	2.5	4.45	4.48	5.53	3.91	5.38
5.845	5.53	4.57	3.13	5.035	4.555	5.575	5.185	5.71
6.475	5.86	5.11	3.565	5.08	4.9	5.95	5.2	5.95
6.895	6.385	5.17	3.73	5.155	5.02	6.01	6.055	6.01
6.94	6.49	5.395	3.775	5.845	5.065	6.88	6.07	6.325
7.465	6.925	5.41	3.85	5.995	5.26	6.955	6.295	6.385
7.495	6.97	5.785	4	6.04	5.275	7.195	6.46	6.7
8.005	7.405	6.13	5.11	6.22	5.89	7.24	6.535	6.715
8.305	7.51	6.19	5.125	6.265	5.92	7.555	6.715	7.075
9.085	7.69	6.43	5.62	6.595	6.1	7.6	7.315	7.36
9.205	7.87	6.445	5.83	6.64	6.34	8.035	7.735	7.405
9.295	7.885	6.535	5.845	6.88	6.67	8.065	7.81	7.54
9.685	8.515	6.82	6.43	7.105	6.7	8.89	7.945	7.6
10.765	8.545	6.865	7.03	7.39	6.97	9.205	8.14	7.975
10.795	9.205	7.135	7.075	7.435	7	9.505	8.185	8.47
11.05	9.22	7.165	7.225	7.69	7.3	9.535	9.31	8.515
12.265	9.895	7.54	7.345	7.825	7.405	10.63	9.385	8.755
12.355	9.925	7.63	7.51	7.87	7.435	10.99	9.715	9.205
13.51	10.645	8.215	7.825	8.725	7.63	11.65	9.73	9.43
13.54	10.84	8.245	7.855	8.905	7.945	11.755	10.825	9.445
13.78	10.87	9.01	8.365	8.95	8.47	11.875	10.87	10.21
13.84	11.05	9.085	8.41	9.1	8.875	12.115	11.395	10.255

High-Purity GB	Low-Purity GB	Surrogate GB	H	Surrogate H	Surrogate VX	VX	WP	TNT
14.995	12.4	9.64	8.725	10.135	8.935	12.7	11.665	10.51
15.16	12.43	10.495	8.83	10.33	9.46	13.03	11.68	10.555
15.475	13.96	10.6	8.86	10.435	9.805	13.72	12.25	11.2
16.195	14.005	11.935	9.16	11.83	9.835	13.78	12.835	11.56
16.405	15.4	12.04	9.385	11.875	10.315	14.005	13.315	12.25
17.065	15.415	12.31	9.43	13.315	10.495	14.08	13.36	12.685
17.635	16.705	13.36	10.24	13.33	10.51	14.38	14.41	13.315
17.8	16.72	13.435	10.33	13.525	11.83	14.41	14.62	13.345
17.845	17.245	13.78	10.405	13.795	11.875	14.935	14.845	13.885
18.355	17.755	14.005	10.915	13.825	12.025	15.835	15.355	14.455
18.385	17.92	14.965	10.93	14.86	13.255	16.06	16.15	15.37
18.97	17.95	15.01	11.785	15.085	13.375	16.105	16.345	15.61
19.51	18.22	15.565	11.83	15.145	13.675	17.68	16.375	16.51
20.02	18.28	16.405	11.935	15.4	13.735	17.95	16.48	16.555
20.605	18.31	17.11	13.18	15.43	13.885	19.24	17.02	17.65
21.37	18.58	17.215	13.42	16.21	14.83	19.285	17.95	17.695
21.715	19.15	17.5	13.435	16.6	15.025	19.465	17.965	18.85
22.945	19.42	18.385	13.555	16.645	15.055	19.81	18.295	19.945
24.31	19.78	18.46	14.755	17.05	15.37	20.59	18.325	20.11
25.855	20.425	18.67	14.995	17.11	16.42	20.875	18.835	21.145
26.965	20.92	18.76	15.19	18.625	16.495	21.01	19.45	21.325
28.06	22.165	20.05	15.25	20.02	16.87	21.22	20.245	22.33
28.63	23.245	25.105	16.96	20.995	17.08	23.425	22.15	22.405
29.755	23.32	26.575	17.035	21.505	18.49	24.73	22.3	23.56
30.355	24.7		17.095	22.9	18.505	26.215	26.065	24.79
	26.41		18.52	24.355	25.705	26.545	26.305	
	26.455		19				30.595	
	26.95		22.63					
	28.48		23.965					
	28.525		30.475					
	30.085							

APPENDIX C

MODIFICATIONS REQUIRED TO MAKE EXISTING ARS SYSTEM FIELDABLE

Based on August 1992 tests at Tooele Army Depot, we have identified the following modifications, both hardware and software, that would be required before the existing ARS system can be considered reliable and fieldable.

The modifications required are also the result of feedback from OSIA inspectors who operated independently one of the ARS systems at Tooele.

C.1 HARDWARE MODIFICATIONS.

- The data-acquisition system needs a logarithmic amplifier for scaling the input signal to prevent amplifier saturation and frequent drive-level adjustment. Will require modification of circuit board.
- The current 14-bit A/D converter needs to be upgraded to 16-bit to provide adequate signal-to-noise and for adequate peak detection. This is particularly important for detecting the lower vibrational modes. Will involve redesign of circuit board.
- Automatic signal drive level (for transmitter transducer) adjustment capability so that operator does not need to manually adjust this.
- Better design for transducer holder and attachment. Other attachment techniques, such as point contact etc., besides magnetic attachment need to be investigated. Most importantly, the total mass of the transducer holder needs to be reduced.
- Single-element transducer design should be studied for improvement in measurement repeatability. This could replace the current two-transducer system and provide better accessibility to munitions because of the resulting smaller transducer holder.
- Incorporation of battery usage and level indicator and warning. The battery powering the ARS circuit board can be monitored by the internal data-acquisition circuitry, and the results can be displayed on screen.
- Extension of the frequency range from the current 1-100 kHz to 0.1 - 200 kHz (or higher). For large structures, the lower frequency will be valuable.
- Faster (19,200 baud) RS232 data transfer capability between the ARS circuitry and computer. This is particularly important for automatic drive-level adjustment and faster sweep. Faster sweep can also be useful for fill level determination in 55-gallon drums.
- Complete redesign of various connectors and cables. This caused us most of the problems at Tooele.

- Miniaturization and weight reduction of signal amplifier close to the receiver transducer for driving long cable. This will also help reduce the total weight of the transducer holder.
- The current ARS circuitry uses reasonably low power, and the system can be operated by a solar-cell power pack, if necessary. In emergency, the solar-cell power pack can be used to recharge batteries.
- Design system such that it is completely operable by a single person. This will require a study of the packaging, such as possibly combining everything, including the computer, into a single box.
- Most annoying feature encountered at Tooele was the difficulty in entering information into the computer with gloves on. Voice recognition system for data (munition specific information, etc.) entry and data-acquisition should be studied. These circuit boards are commercially available. Also audible feedback to operator is necessary when problems, such as bad transducer contact, broken cable, questionable munitions etc., occur.
- Miniature head-mounted video display was demonstrated at Tooele. This could be incorporated into the system for providing operator feedback as well.

C.2 SOFTWARE MODIFICATIONS.

- Multiple frequency range selection and operation capability in a single sweep. This range can be selected automatically based on munition being tested.
- Algorithm requires fluid-level fluctuation correction to improve reliability of munition identification.
- Loading effect (when munitions are piled on top of each other in many rows) corrections also need to be incorporated in the identification algorithm.
- Corrections for temperature variation.
- Corrections for variations in physical properties within the same class, e.g., low purity vs. high purity, stratification, sedimentation, etc.
- Statistical analysis of data to derive proper confidence levels.
- The present correlation algorithm requires a significant amount of improvement to enhance reliability. The current algorithm does not take into account the amplitude and Q of resonance peaks. These parameters, in addition to the resonance frequencies, need to be incorporated.
- Algorithm to extract munition configuration-dependent features from the data needs to be developed. This will allow unknown munition types to be studied by the ARS technique. We have identified certain geometry-dependent features from our Tooele data that require further study.
- Finally, algorithm for the determination of agent physical properties, such as speed of sound, density, and viscosity, need to be worked on further. The present algorithm

does not appear to be adequate for the purpose. May require more model studies. *Our original program did not require us to do this.*

- Technique for liquid-level determination in 1-ton containers needs to be developed. This will require both modeling and physical model studies. Currently, we can easily distinguish between GB and H-filled 1-ton containers regardless of fill variation, but we cannot determine fill level (*we never promised to be able to do this either*).

ACOUSTIC RESONANCE SPECTROSCOPY SYSTEM

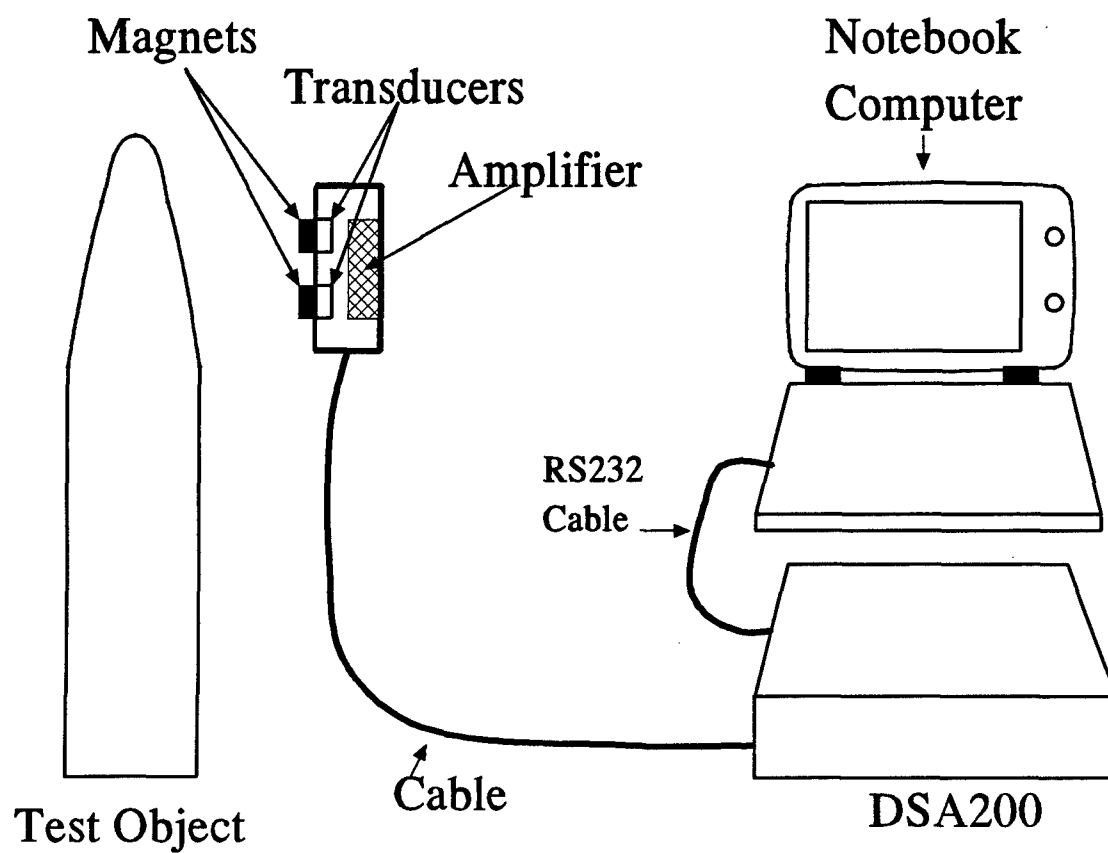


Figure 1. Acoustic Resonance Spectroscopy System.

LOS ALAMOS NATIONAL LABORATORY
ACOUSTIC RESONANCE SPECTROSCOPY SYSTEM

--- SELECT ARS OPERATIONS---

⇒ *General Information Input*

Calibrate System

Acquire template Data

Take Normal Data

Set Status

Display Stored Data

Exit Program

PLEASE ENTER INFORMATION BEFORE BEGINNING SESSION

Figure 2. ARS Operation Selection Menu.

LOS ALAMOS NATIONAL LABORATORY General Information Input for ARS Measurements			
First Operator:	Dipen N. Sinha	Org.	Los Alamos
Second Operator:	Kendall Springer	Org.	Los Alamos
Test Location	Tooele Army Depot	Temperature (F)	85
Site	South	Igloo (Bldg.)	XXXX
Date	09/23/92	Munition Type	155-mm GB
General Information: (3 lines)		Production lot:	
Munitions Stacked horizontally Munitions are in pallet but not touching each other Munition surface extremely dirty and covered with a lot of dust			
Drop-Down, Scrollable Window for munition selection from list <div style="text-align: center; margin-top: 10px;"> </div>		<div style="text-align: center; margin-bottom: 5px;"> </div> <div style="font-family: monospace;"> Spray Tank 105-mm GB 155-mm GB Low Purity 155-mm GB High Purity 155-mm H (Mustard) 155-mm VX 155-mm HE 155-mm White Phosphorus 1-Ton H (Mustard) 1-Ton GB MC-1 GB (Unknown) 105-mm Surrogate-P HD 105-mm Surrogate-P GB 105-mm Surrogate-P VX 55 Gallon Drum 1-Ton Empty </div>	

Operator Interface Used at Tooele for Information Entry

Figure 3. General Information Input Screen.

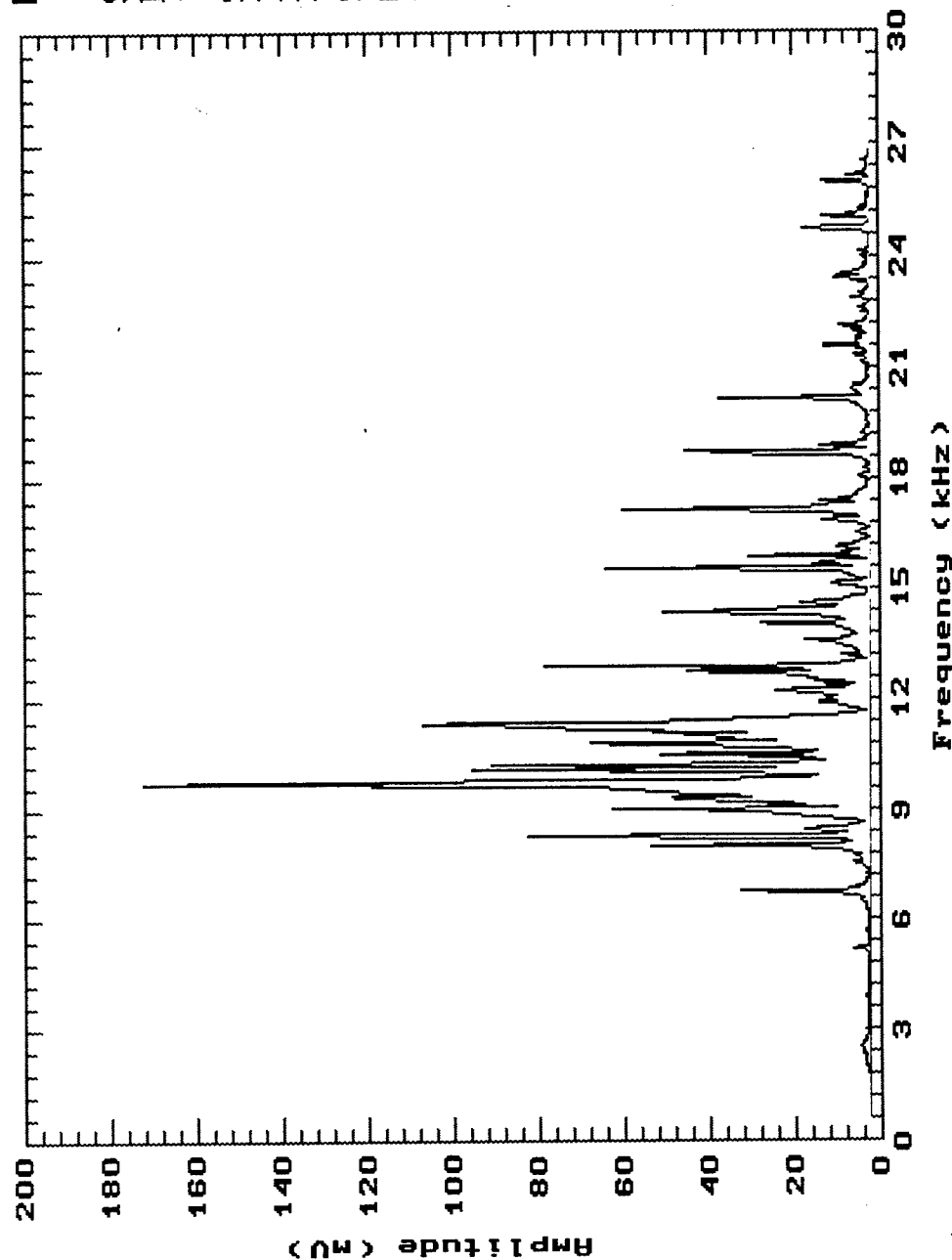
RUNNING COUNTER

DSA200: HOMODYNE

10-08-1992
13:40:14

HOMODYNE

Start
Frequency:
1000 Hz
Stop
Frequency:
30000 Hz
Sweep
Amplitude:
3 V-pk
Sweep point:
291 pts
Sweep step:
100 Hz
Sweep Rate:
20 step/s
Sweep Time:
15 sec
Full scale:
200 mV



★★★★ RESULTS ★★★★★

RESTORE (F1) EDIT (F2) SWP OFF(F3) EXIT (F4) SCALE (F5)

Figure 4. Graphical Display Screen During ARS Measurement.

TEMPLATE GENERATION PROCESS

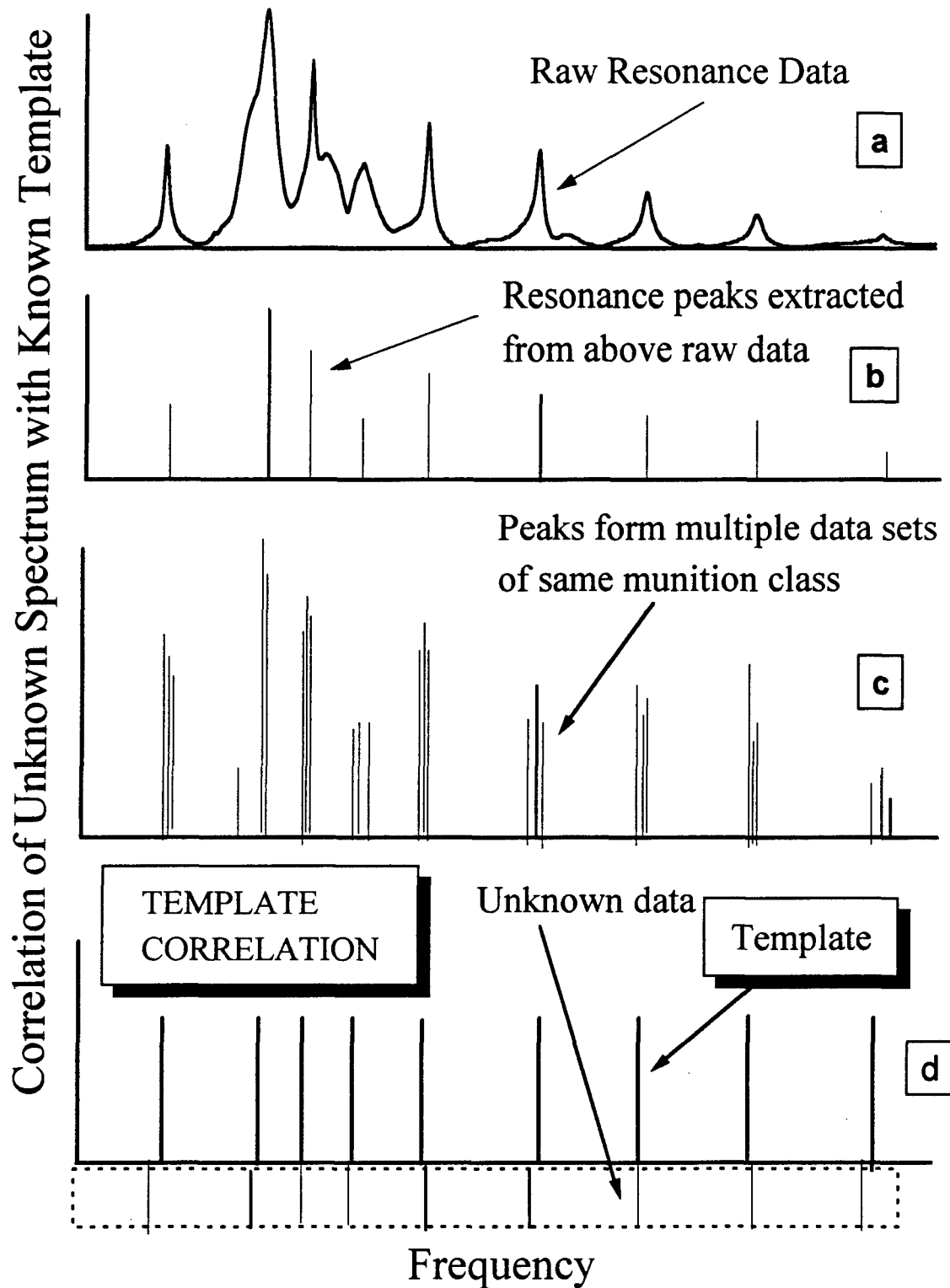


Figure 5. Graphical Representation of Template Generation Process.

Comparability of Data Within Class

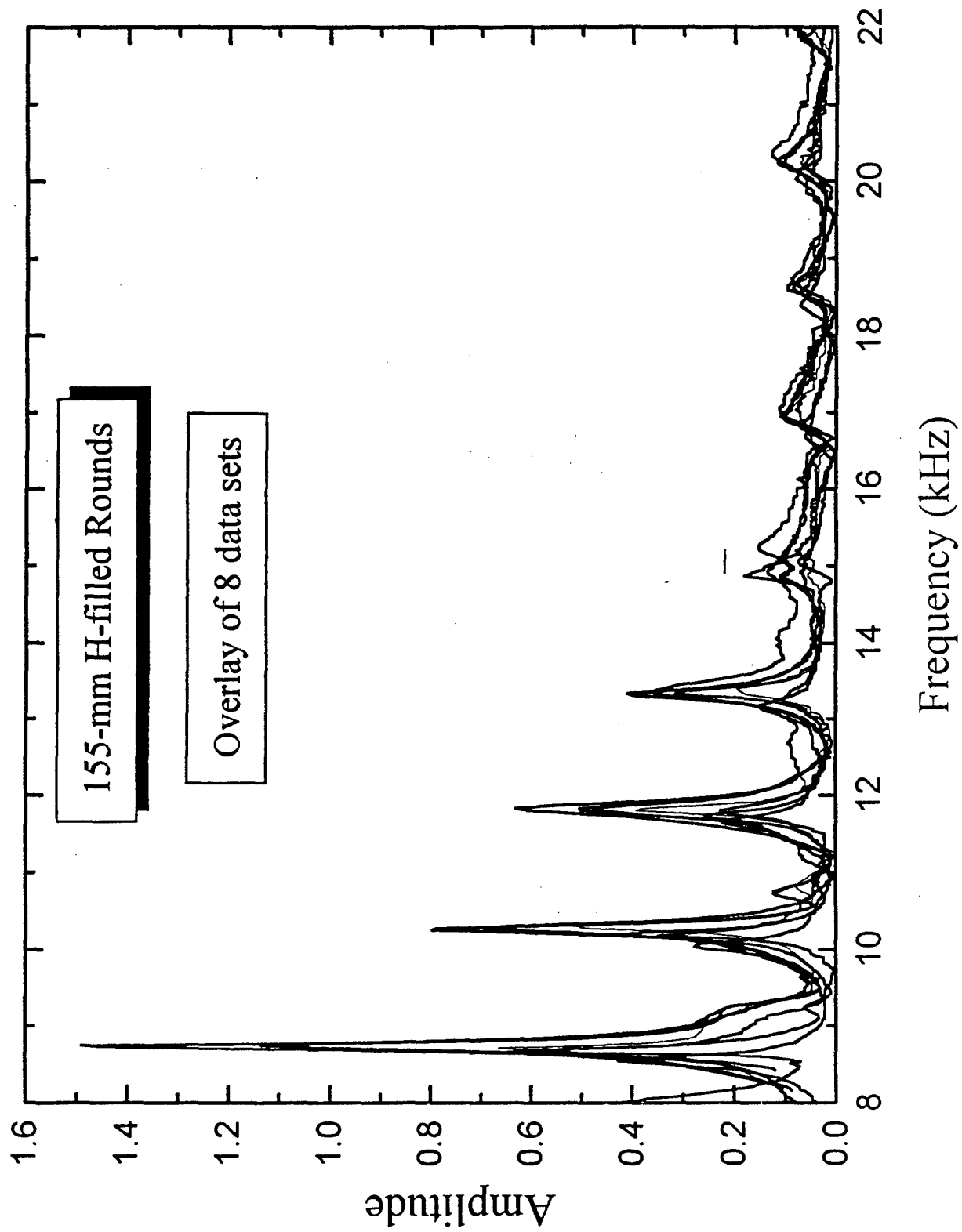


Figure 6. Comparability of Data Within a Given Class of Munitions.

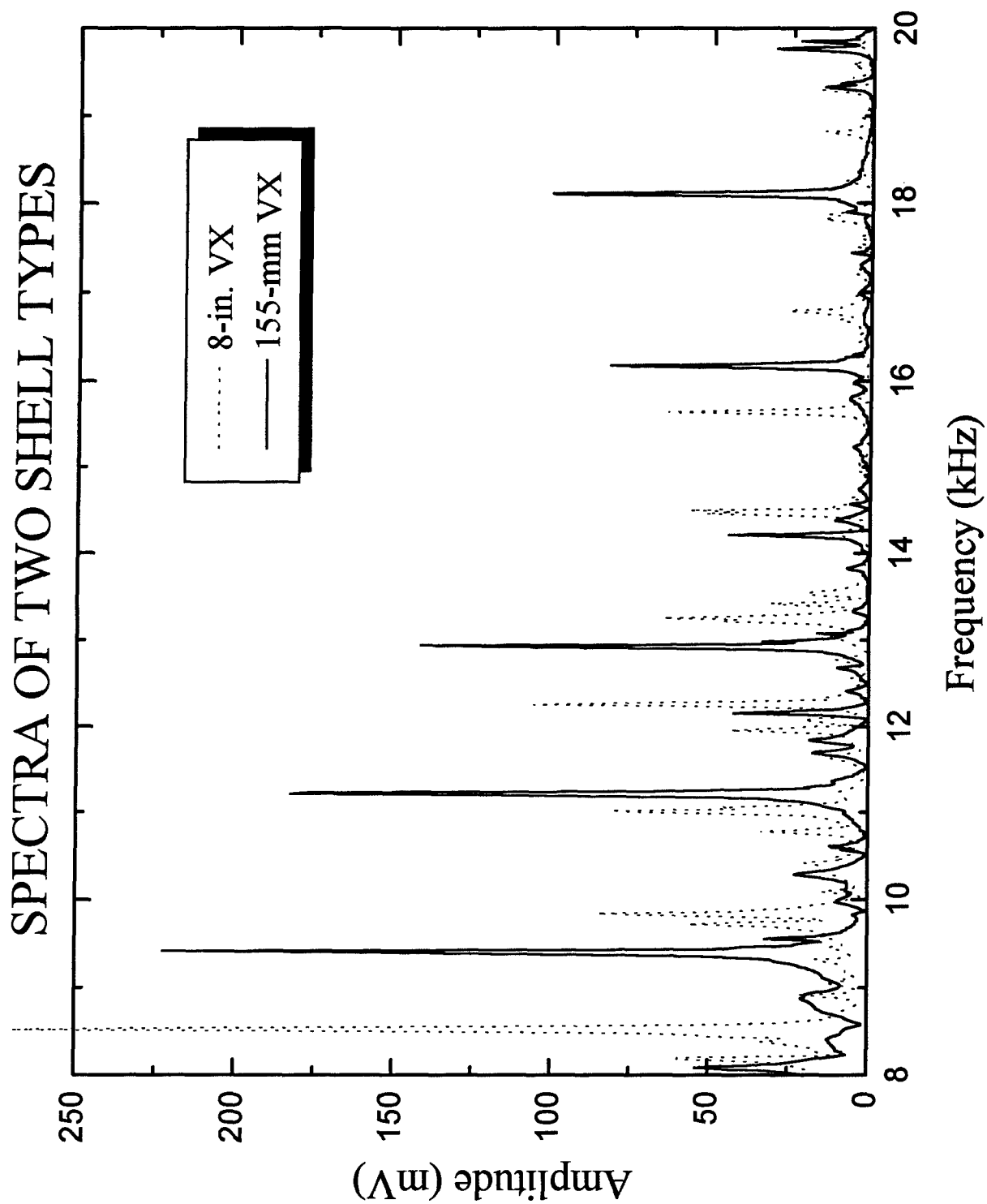


Figure 7. Comparison of Spectra Between Two Shell (Munitions) Sizes.

ACOUSTIC SPECTRA OF 155-mm ROUNDS

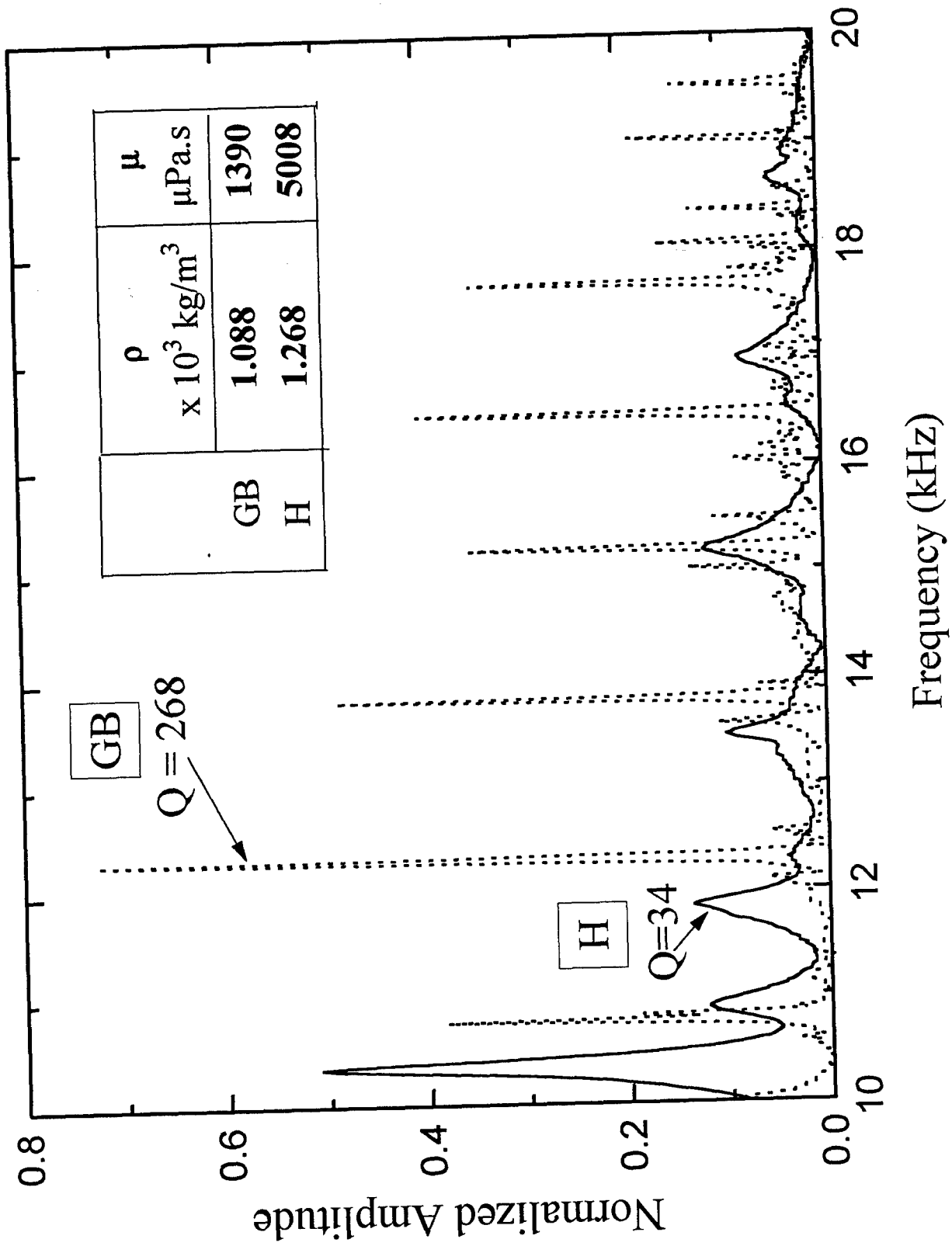


Figure 8. Comparison of Spectra Between H- and GB-Filled Rounds.

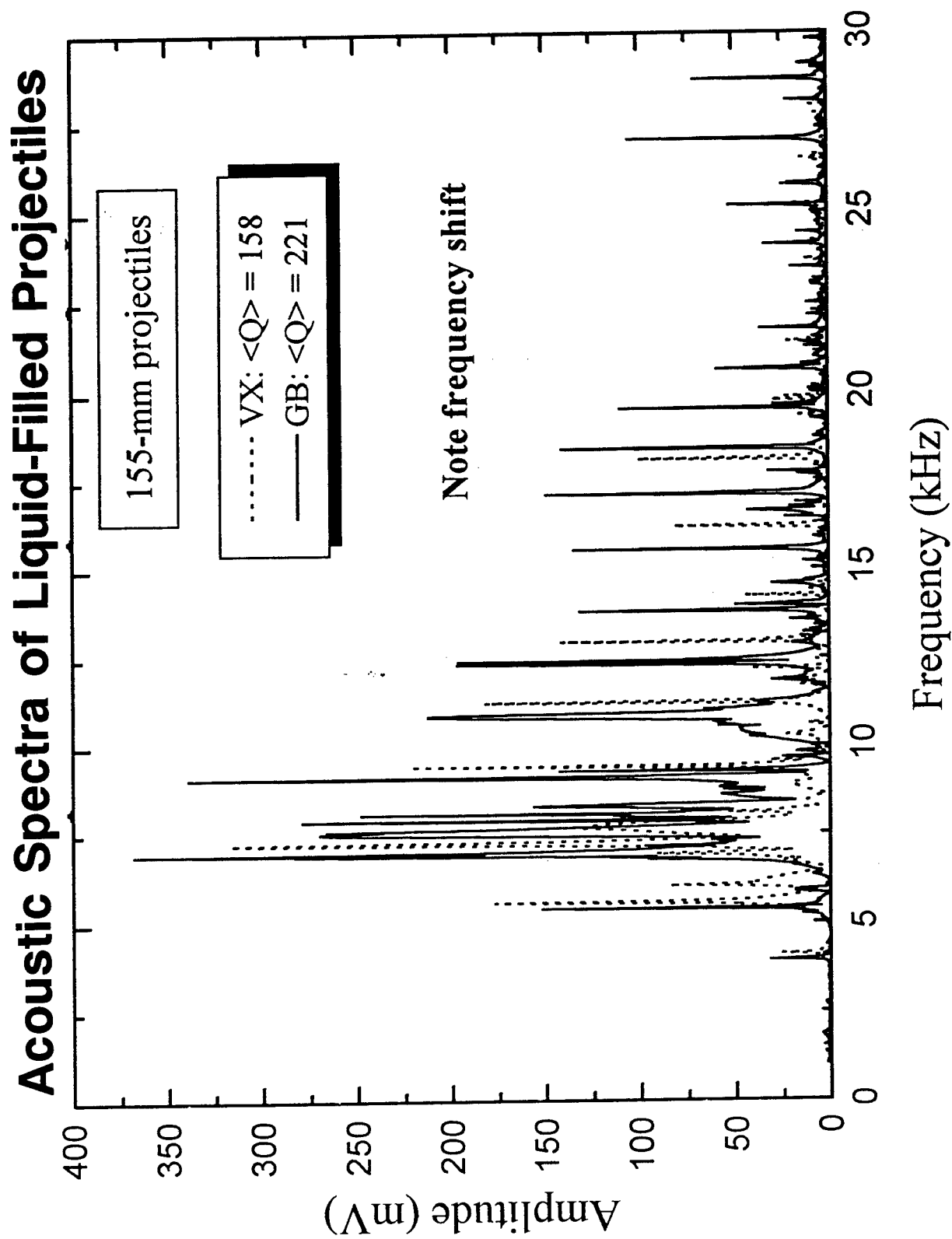


Figure 9. Comparison of Spectra Between VX- and GB-Filled Rounds.

Acoustic Spectra of 1-Ton Containers

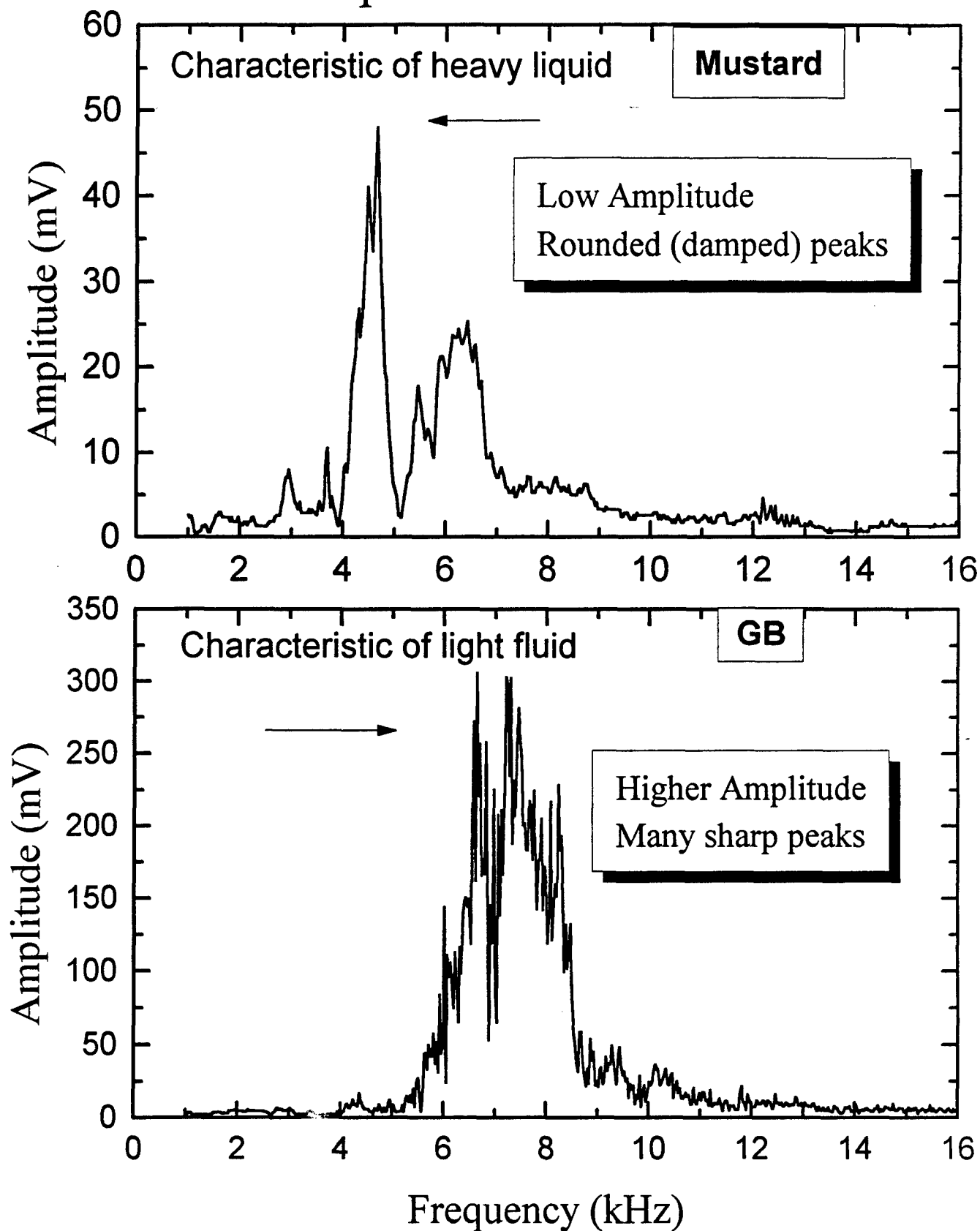


Figure 10. Comparison of 1-ton Container Spectra (Mustard and GB Fill).

Histogram of Number of Resonance Peaks

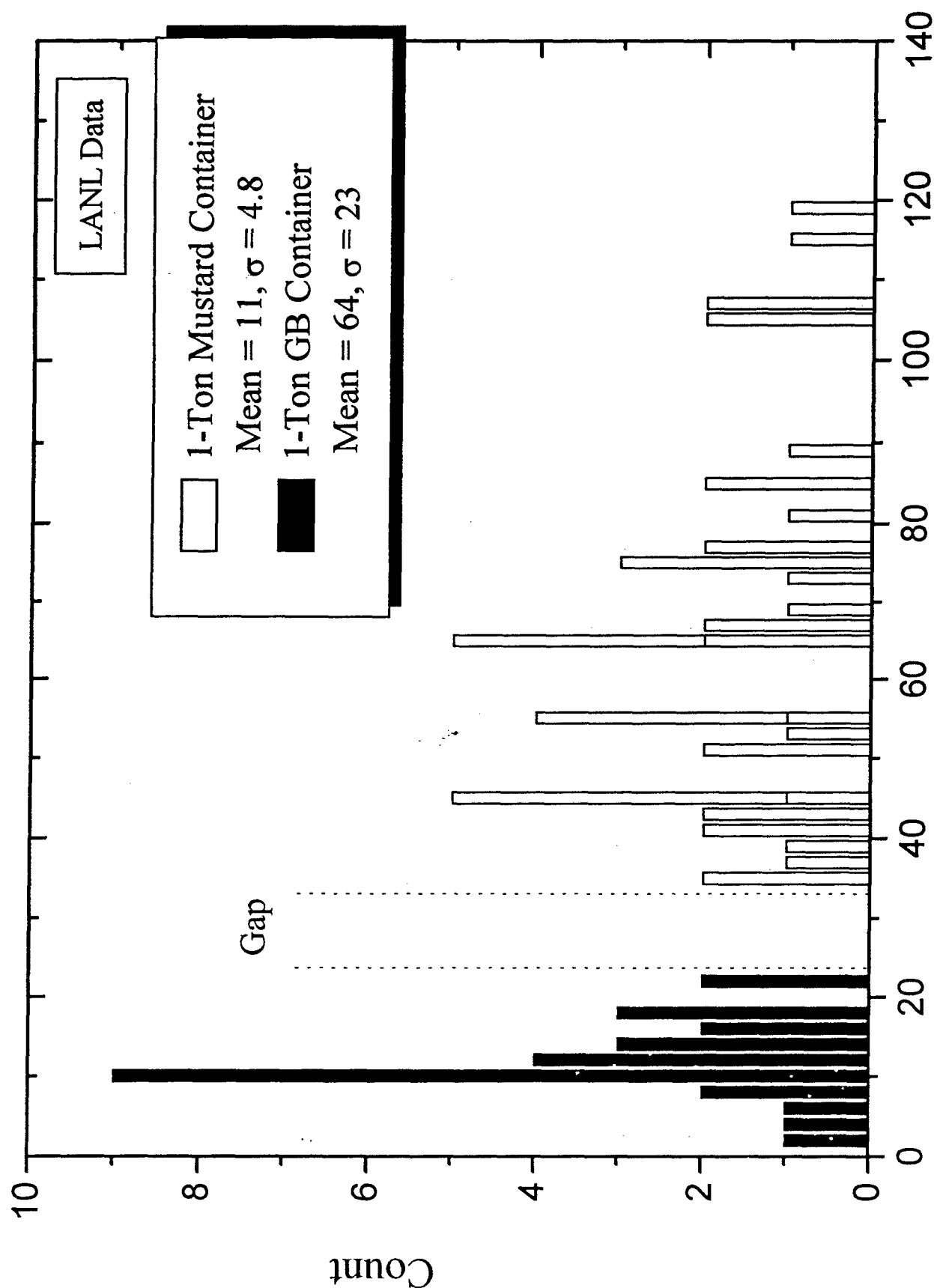


Figure 11. Histogram of Data Shown in Figure 10.

Characteristics of 1-Ton Container Spectra

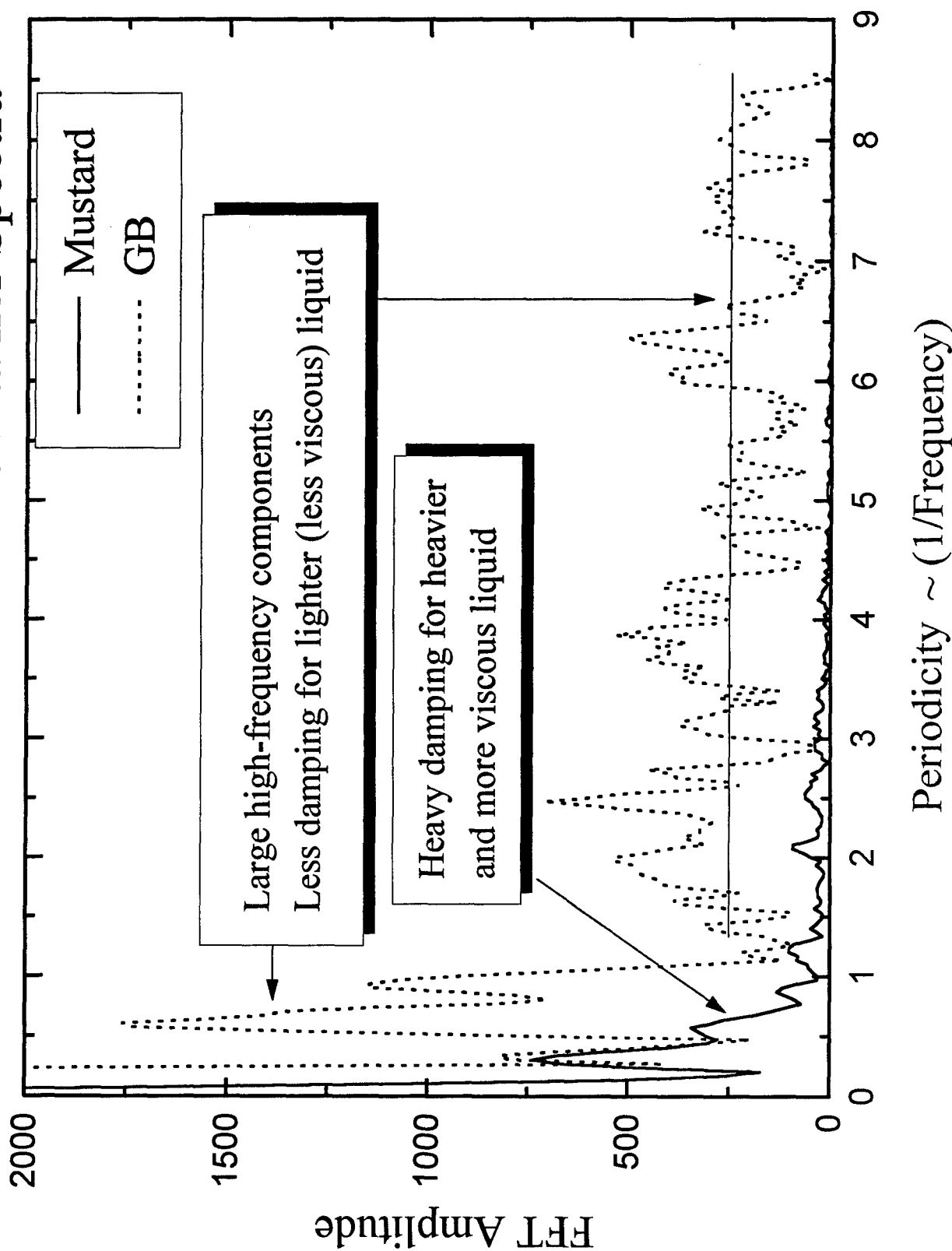


Figure 12. Comparison of Fourier Transform of 1-ton Container Spectra.

Acoustic Spectrum of MC-1 Bomb GB

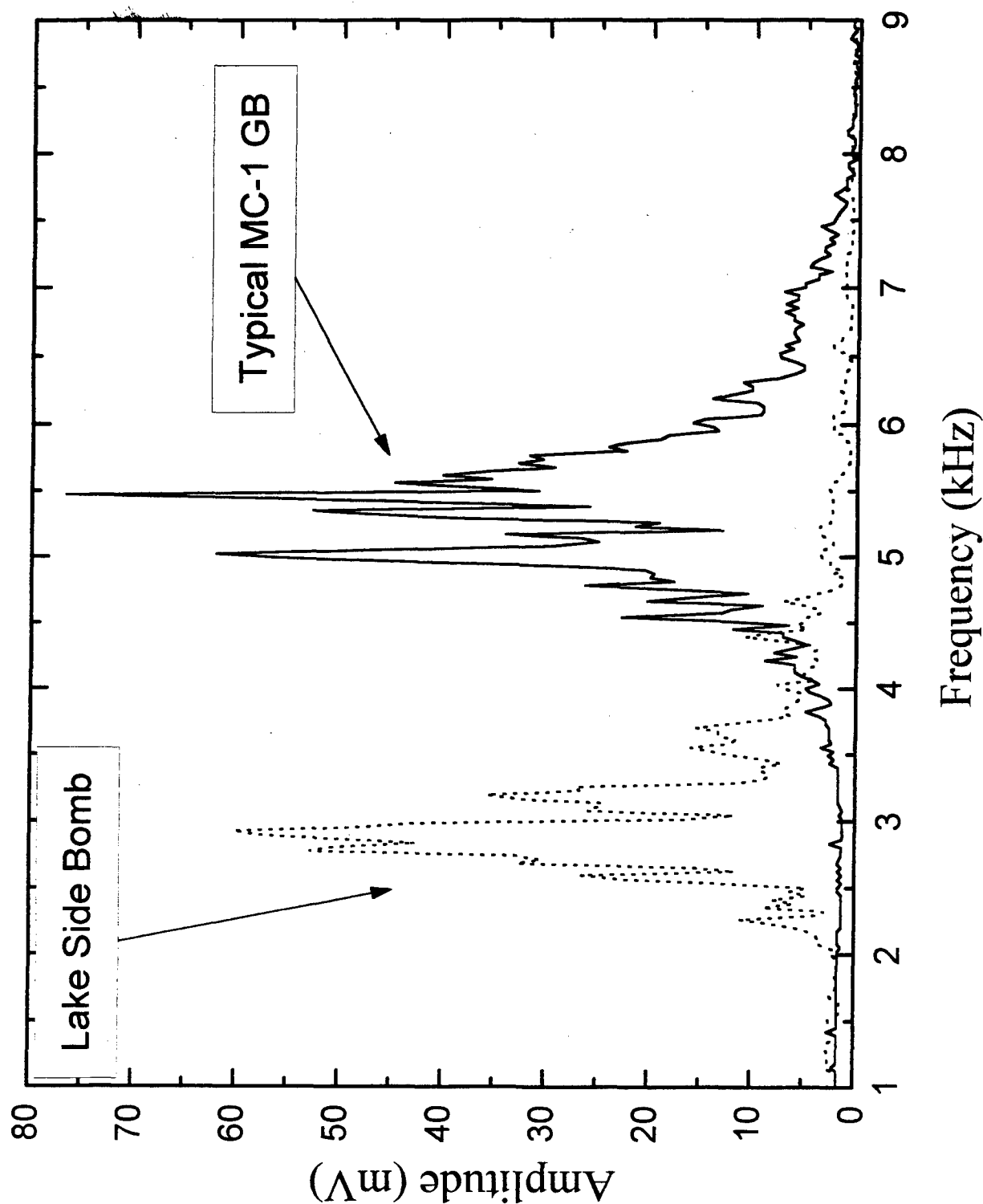


Figure 13. Typical Spectra of GB-Filled MC-1 Bomb.

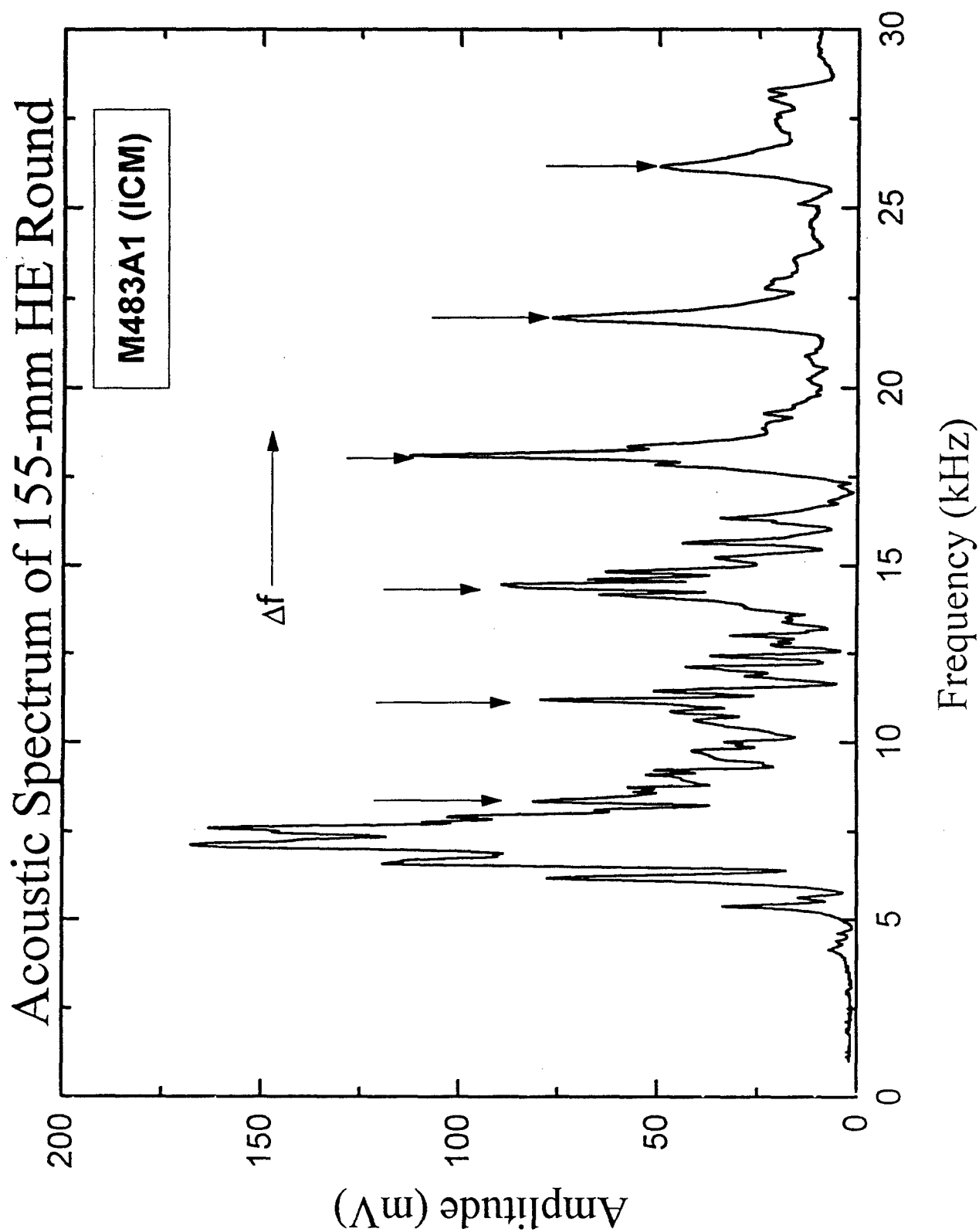


Figure 14. Typical Spectra of HE-Filled 155-mm ICM.

Acoustic Spectrum of VX Spray Tank

Measurements made on the container from outside. Filled tank inside loads the structure and shifts frequencies to lower values. Amplitudes are also significantly lower for same level of excitation.

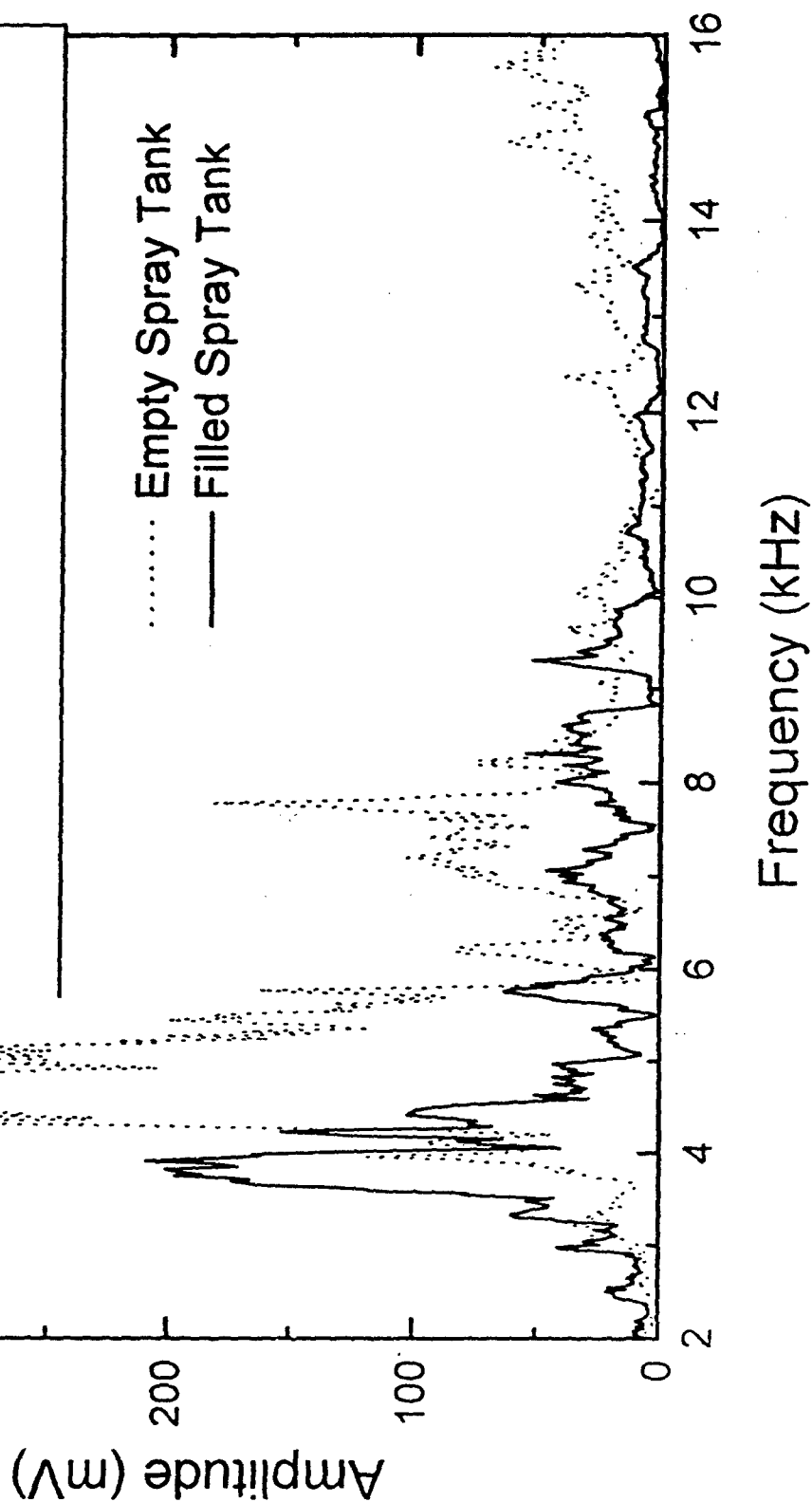


Figure 15. Typical Spectrum of VX Spray Tank (Effect of Weight).

Typical Spectrum of HE-Filled M107 Round

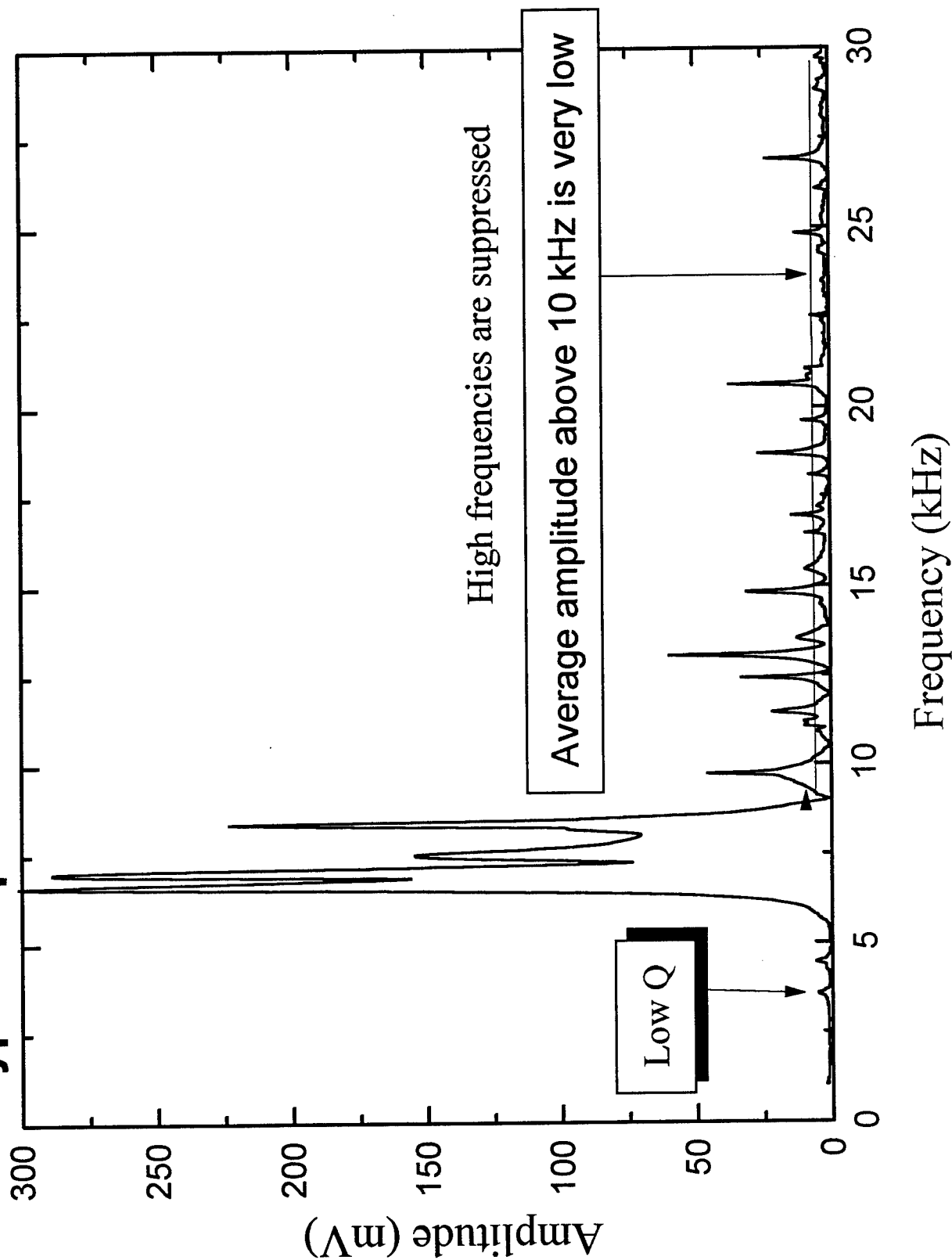


Figure 16. Typical Spectrum of HE (solid)-Filled Rounds.

Acoustic Spectrum of 155-mm GB Round

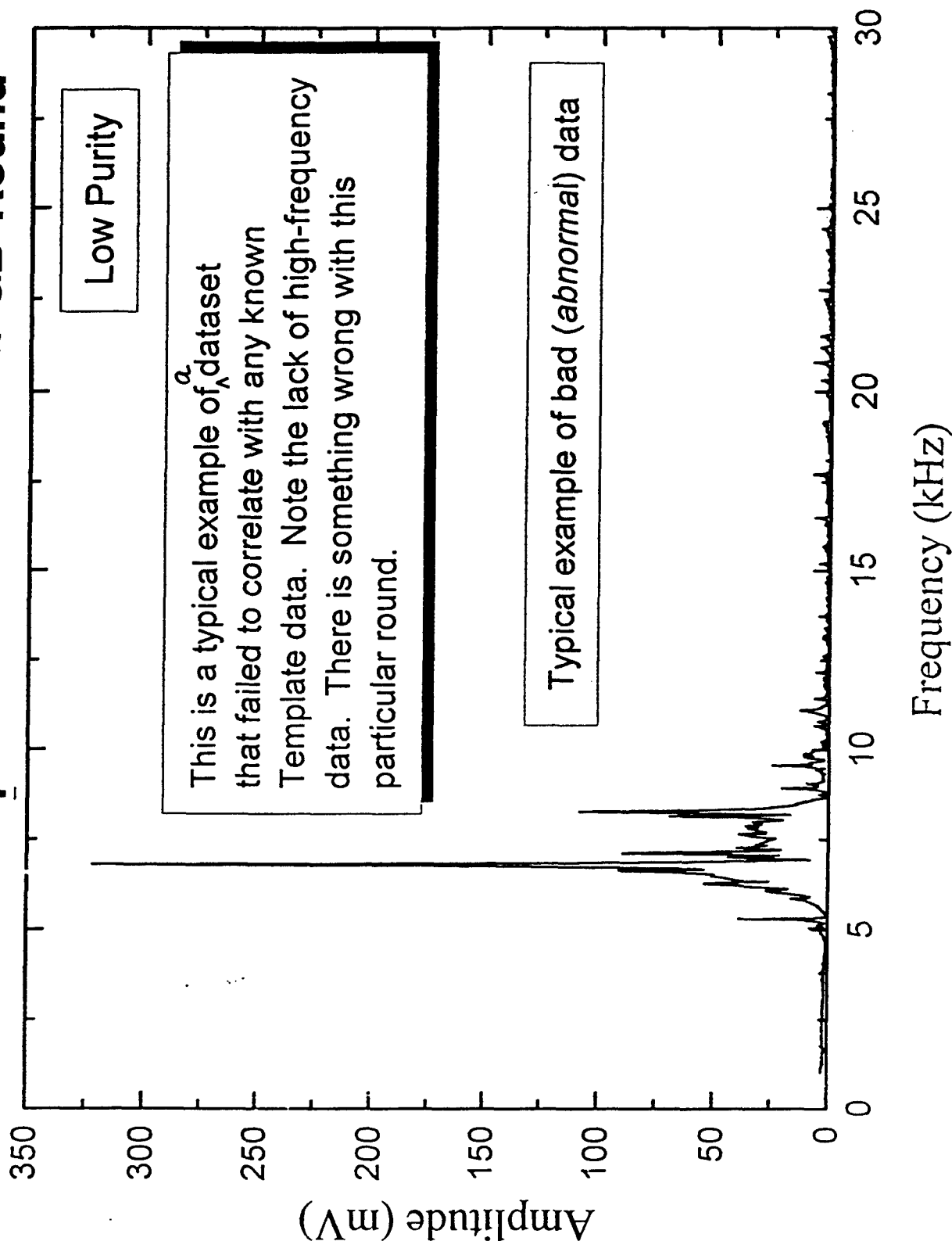
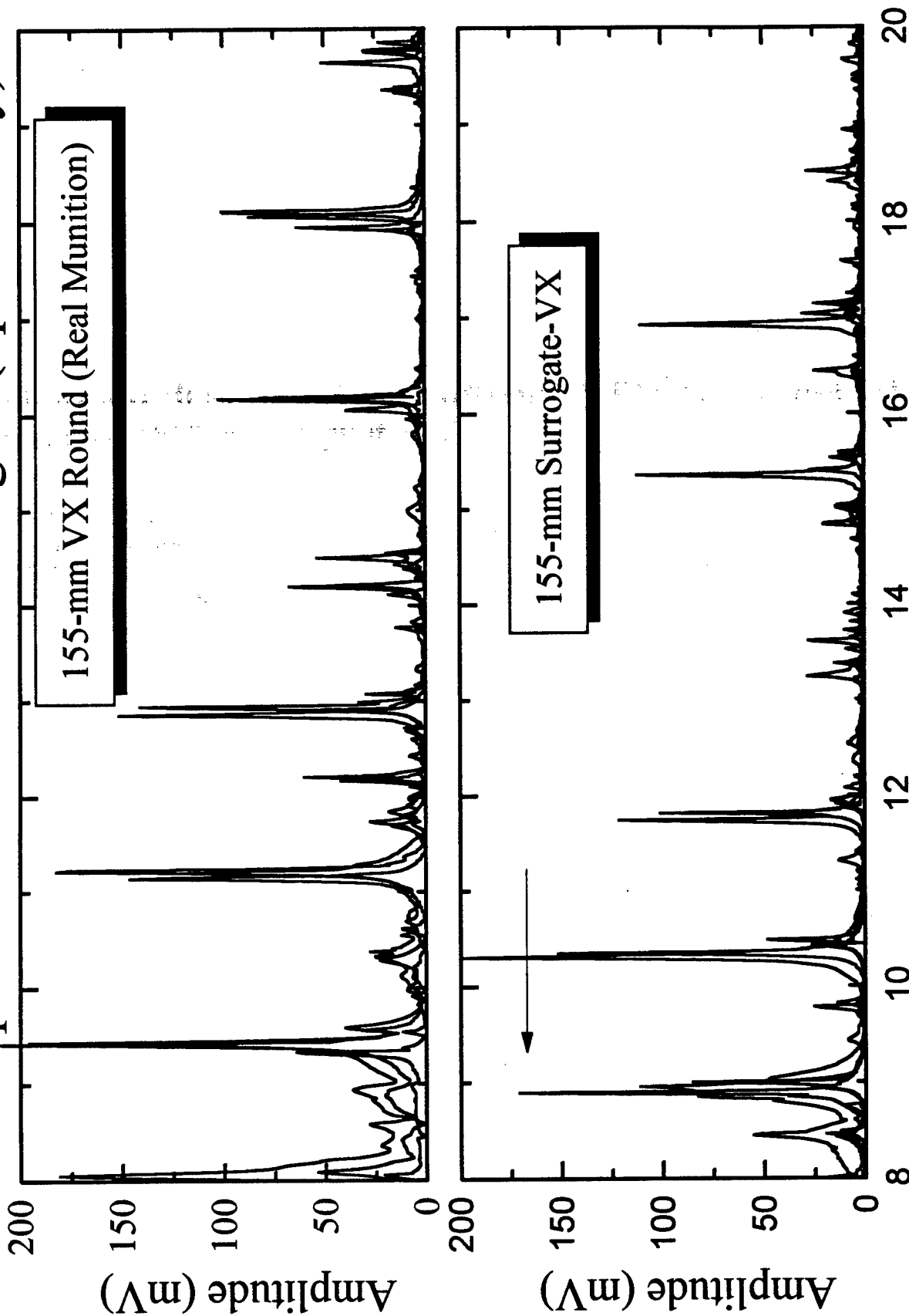


Figure 17. Example of Abnormal Data.

Comparison of Real vs. Surrogate (Spoofability)



Frequency (kHz)

Figure 18. Comparison of Real (VX) vs. Surrogate-Filled Munitions.

COMPARISON OF SURROGATE VS. REAL

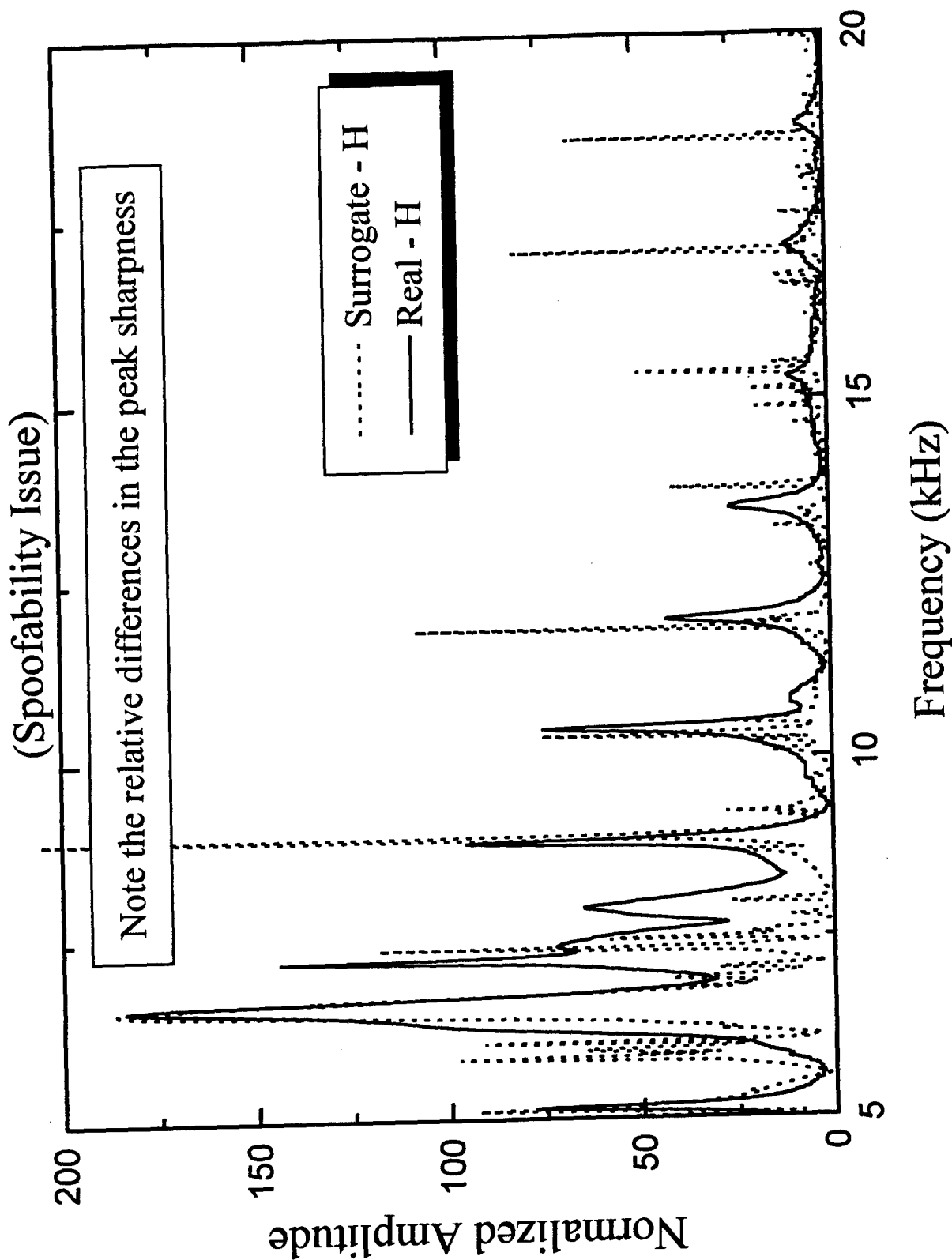


Figure 19. Comparison of Real (H) vs. Surrogate-Filled Munitions.

DISTRIBUTION LIST

DNA-TR-93-84

DEPARTMENT OF DEFENSE

DEFENSE NUCLEAR AGENCY
5 CY ATTN: R JOHNSTON OPAC
2 CY ATTN: TITL

DEPARTMENT OF THE ARMY

DUGWAY PROVING GROUND
3 CY ATTN: STEDP-JCP/DR CLARKE

U S ARMY CHEMICAL RSCH & DEV CTR
5 CY ATTN: SMCCR-MUM (DR HUTCHINSON)

DEPARTMENT OF ENERGY

DEPARTMENT OF ENERGY
5 CY ATTN: DP-5.1 G DUDDER

LOS ALAMOS NATIONAL LABORATORY
2 CY ATTN: D N SINHA
5 CY ATTN: DR K E APT

DEPARTMENT OF DEFENSE CONTRACTORS

JAYCOR
ATTN: CYRUS P KNOWLES

KAMAN SCIENCES CORP
ATTN: DASAC

KAMAN SCIENCES CORPORATION
ATTN: DASAC

SCIENCE APPLICATIONS INTL CORP
12 CY ATTN: CVR MR FARGO



Defense Threat Reduction Agency

8725 John J Kingman Road MS 6201
Ft Belvoir, VA 22060-6201

TDANP-TRC

August 1, 2001

MEMORANDUM TO DEFENSE TECHNICAL INFORMATION CENTER
ATTN: OCQ/MR LARRY DOWNING

SUBJECT: DOCUMENT CHANGES

The Defense Threat Reduction Agency Security Office reviewed the following documents in accordance with the Deputy Secretary of Defense Memorandum entitled, "Department of Defense Initiatives on Persian Gulf War Veterans' Illnesses" dated 22 March 1995, and determined that the documents were unclassified and cleared for public release:

DNA-TR-93-84, AD-B244408, Acoustic Resonance Spectroscopy in CW Verification Tooele Field Trial (August 1992).
DNA-TR-93-129-V1, AD-B192045, Global Proliferation – Dynamics, Acquisition Strategies and Responses, Volume 1 – Overview.
DNA-TR-93-129-V2, AD-B192046, Global Proliferation – Dynamics, Acquisition Strategies and Responses, Volume 2 – Nuclear Proliferation.
DNA-TR-91-216, AD-B163637, Harmonizing the Chemical Weapons Convention with the United States Constitution.
DNA-TR-92-180, AD-B175230, Evaluation of the Concept of a List for the BWC.
DNA-TR-92-61, AD-B167663, Basic State Party Functions and Skills Under CWC.
DNA-TR-92-66, AD-B167357, Domestic Reporting Requirements for Chemical Industry.
DNA-TR-91-213, AD-B163260, Analysis of the Interactions Between Treaties.
DNA-TR-93-70, AD-B177262, Chemical Weapons Convention Inspections of Private Facilities Application of United States Environmental and Safety Laws.
DNA-TR-92-182, AD-B173450, Commercial Products from Demilitarization Operations.
DNA-TR-91-217-V3, AD-B169350, Chemical Weapons Process Parameters, Volume 3 – Users' Guide.
DNA-TR-92-116-SUP, AD-B175292, Technical Ramifications of Inclusion of Toxins in the Chemical Weapons Convention (CWC), Supplement.
DNA-TR-92-128, AD-B175452, Task 1 Report Target Vapor Identification and Database Development.
DNA-TR-92-196, AD-B174940, Task 2 Report Algorithm Development and Performance Analysis.
DNA-TR-93-68, AD-B178109, CW Detection Instrument R&D Design Evaluation.

Enclosed is a copy of the referenced memorandum. If you have any questions, please call me at 703-325-1034.

Arndith Jarrett
ARDITH JARRETT
Chief, Technical Resource Center